Heliyon 10 (2024) e26784

Contents lists available at ScienceDirect

Heliyon

journal homepage: www.cell.com/heliyon

Review article

An overview of techniques for monitoring and compensating tool wear in micro-electrical discharge machining

Rahul Nadda [a], Chandrakant Kumar Nirala [b,**], Prashant Kumar Singh [c], Daeho Lee [d], Raj Kumar [d,f], Tej Singh [e,*]

[a] Department of Biomedical Engineering, Indian Institute of Technology Ropar, Punjab, 140001, India
[b] Department of Mechanical Engineering, Indian Institute of Technology Ropar, Punjab, 140001, India
[c] Department of Mechanical Engineering, Invertis University, Bareilly, UP, 243123, India
[d] Department of Mechanical Engineering, Gachon University, Seongnam, 13120, South Korea
[e] Savaria Institute of Technology, Faculty of Informatics, ELTE Eötvös Loránd University, Budapest 1117, Hungary
[f] Faculty of Engineering and Technology, Shoolini University, Solan, H.P., 173229, India

ARTICLE INFO

Keywords:
EDM
Tool wear compensation
Offline compensation
Micro EDM
Online compensation

ABSTRACT

Micro-electrical discharge machining (μEDM) is severely affected by tool wear and its process variants, which can lead to compromised precision and dimensional disruptions in micro-part production. Several attempts have been made to address this problem by suggesting offline and online (real-time) tool wear compensation strategies. Research efforts in this area have intensified over the last 20 years. However, most methods proposed were applicable only for a few work-tool combinations and in limited input process parametric settings. Instead of tool wear compensation, several research articles have focused on strategies to reduce the negative impact of tool wear on the quality of fabricated parts. The present study systematically reviews various investigations conducted in this area and aims to add cutting-edge compensation for tool wear to future inquiries. The articles reviewed here are explored in detail. Critical findings/innovations are classified into four categories: tool wear in μEDM, tool wear compensation techniques, and offline and online compensation methods.

1. Introduction

In the current highly competitive manufacturing industry, achieving dimensional precision of micro-parts and reducing machining time are two crucial requirements for successful micro-manufacturing [1]. Therefore, precision machining is an essential technology for producing microscopic parts and features. Micromachining is a well-known machining category with the capability to manufacture different sizes of components ranging from 1 μ m to 999 μ m, or the amount of material being removed is measured in microns [2]. The desire for products fabricated from robust engineering materials has forced researchers to consider new manufacturing routes. Due to their superior material and mechanical properties, the requirement for micro components with advanced materials like ceramics, super alloys, and composites has recently increased. Researchers have identified various applications for these materials in engineering, automobiles, aerospace, and biomedical industries. The hardness, high toughness, and fatigue of sophisticated and exceptional

* Corresponding author.
** Corresponding author.
E-mail addresses: nirala@iitrpr.ac.in (C.K. Nirala), sht@inf.elte.hu (T. Singh).

https://doi.org/10.1016/j.heliyon.2024.e26784
Received 13 June 2023; Received in revised form 17 February 2024; Accepted 20 February 2024
Available online 29 February 2024

Nomenclature

C	Combination of a fraction of energy and a fraction of molten region area
CNC	Computer numerical control
CCD	Charge-coupled device
E	Complete elliptic integrals of the second kind
EWC	Electrode wear compensation
EWR	Electrode wear rate
erfc	Complementary error function
HAR	High aspect ratio
IEG	Inter electrode gap
I_a	Average current (A)
K_t	Average thermal conductivity ($Wm^{-1}K^{-1}$)
K	Complete elliptic integrals of the first kind
LIGA	Lithographie, Galvanik and Abformung (German word)
LCM	Linear compensation method
MRR	Material removal rate
PSD	Power spectral density
q	Heat flux (Wm^{-2})
r	Radial distance of material (μ m)
R	Heat flux radius (μ m)
SR	Surface roughness
SEM	Scanning electron microscopy
T	Temperature (K)
T_{on}	Pulse on time (ns)
TWC	Tool wear compensation
UWM	Uniform wear method
V_a	Average voltage (V)
w	Vertical distance towards cathode and heat flux radius
μEDM	Micro-electrical discharge machining
μLBM	Micro laser beam machining
μEBM	Micro electron-beam machining
u	Radial distance of material to heat flux radius in the vertical axis

Greek Letters

α	Average thermal diffusivity (m^2s^{-1})
τ	Different instants of time

materials make them challenging to machine. Therefore, non-conventional micromachining methods are an essential family of technologies that can facilitate the production of micro parts.

The term non-conventional micromachining methods refers to manufacturing techniques that deviate from conventional methods in micromachining. These methods often involve innovative or unconventional approaches to achieve precision machining at a microscale. Non-conventional methods include laser ablation, electrochemical machining, μEDM, and focused ion beam machining. These techniques differ from traditional machining processes like milling or turning and are particularly suited for intricate micro-scale fabrication where high precision and intricate geometries are required. Non-conventional machining methods utilize different energy forms like chemical, optical, mechanical, electrical, and thermal to remove materials, diverging from the conventional machining approach that relies on sharp-edged cutting tools. Table 1 outlines several key features, capabilities, and applications of micro-machining techniques. μEDM is a commonly used non-conventional micromachining method to manufacture micro-components on advanced materials because of its capability to deal with electrically conductive, tough, and brittle materials independent of their mechanical qualities.

During μEDM, the electrode and workpiece are kept apart, which results in minimum mechanical stresses, debris, and vibration issues in the manufacturing process. With its numerous benefits, μEDM can produce holes with a diameter as small as 10 μm and blind holes with an aspect ratio of up to 20 μm [9]. Micro-EDM produces minute sparks lasting around 50 ns and a small electric current of 0.25A, resulting in minimal input energy per discharge and a low material removal rate per unit [12,13]. Furthermore, μEDM offers lower setup costs, ample design freedom, a large aspect ratio, and improved accuracy compared to other competing methods like Lithographie, Galvanik, and Abformung (LIGA), micro laser beam machining (μLBM), and micro electron-beam machining (μEBM). While electrode size and shape may vary, the material removal mechanism in micro-EDM exhibits comparable behavior to conventional EDM, with the primary distinction in the quantity of input energy delivered. Both the specimen and electrode are attached to a suitable DC power supply. Based on open-circuit voltage, an inter-electrode gap (IEG) is maintained among the specimen and electrode

Table 1
Micromachining variants with their capabilities and applications.

Variant	Source of energy	Capabilities of variant	Applications
Electrochemical micromachining [4,5]	Thermal and Chemical	- 3D, voltage = 1–10 V - Inter electrode gap = 5-50 μ m - R_a = 0.05–0.4 - Accuracy = ± 0.01 mm	- Deburring - Print bands finishing - Nozzle plate for inkjet printer head
Electrochemical jet machining [6]	Thermal and Chemical	- 3D, voltage = 150–170 V - Pressure = 0.3–1.0 MPa - Electrolyte = 10–25%	- Drilling of holes
Micro EBM [7,8]	Electromagnetic	- $Width_{min}$ = 25 μ m - Density = 6500 GW/mm^2 - Energy range = 10–1000 eV	- Drilling of various materials - Holes in wire drawing dies - Cooling holes in turbine blades
μEDM die sinking [3]	Thermal	- R_a = 0.50 μ m - 3D, $Width_{min}$ = 20 μ m - Aspect ratio = 20	- Replication molds - Coinage die making - Prototype production
μEDM milling [3]	Thermal	- 3D, $Width_{min}$ = electrode diameter - R_a = 0.50 μ m	- Micro-injection molds - Embossing or coining tools
Abrasive slurry jet micromachining [9,10]	Mechanical	- 3D, $d_{hole,\ min}$ = 5-9 μ m - $Depth_{min}$ = 37 μ m	- Coating and metal forming - Chemical processing
μEDM drilling [3]	Thermal	- R_a = 0.30 μ m - 2D, $d_{hole,\ min}$ = 40 μ m - Aspect ratio = 25-50	- Injection nozzles
Ultrasonic micromachining [9,11]	Mechanical	- 3D, $d_{hole,\ min}$ = 20 μ m - Frequency = 20–40 kHz - Amplitude = 2-100 μ m	- Press tool dies - Machining of watch bearings and jewels
μWEDM [3]	Thermal	– 2½D, $d_{wire,\ min}$ = 30 μ m - h_{max} = 5 - S_{min} = 40 μ m - R_a = 0.07 μ m	- Opto-electronic components, - Stamping tools
μLBM [9]	Thermal	- 1D, spot size = 0.015–0.075 mm - Beam output = 10–1000 W - Peak power = 100–400 kW	- Small holes>0.25 mm in diameter - Holes up to 1.5 mm - Diameter - Large holes (trepanned) - Drilling (punching/percussion)

throughout the machining. During μEDM, the specimen and electrode are submerged in a dielectric fluid. The presence of a fixed potential difference and IEG is necessary to establish an electric field between the electrode and specimen during μEDM. In EDM, a straight polarity is defined by attaching the negative end to the tool and the positive end to the workpiece. The free electrons within the tool experience electrostatic force due to the electric field between the workpiece and the electrode.

Electrons emitted from the tool electrode accelerate towards the anode in the IEG after an appropriate electric field has been developed. As dielectric molecules fill the gap between the electrode and specimen, collision between electrons and dielectric molecules occurs, causing the molecules to split into electrons and ions. Once the concentration of ions, i.e., positive ions and electrons, exceeds a threshold in the IEG, the workpiece and electrode create a plasma channel due to the avalanche motion of the electrons. This

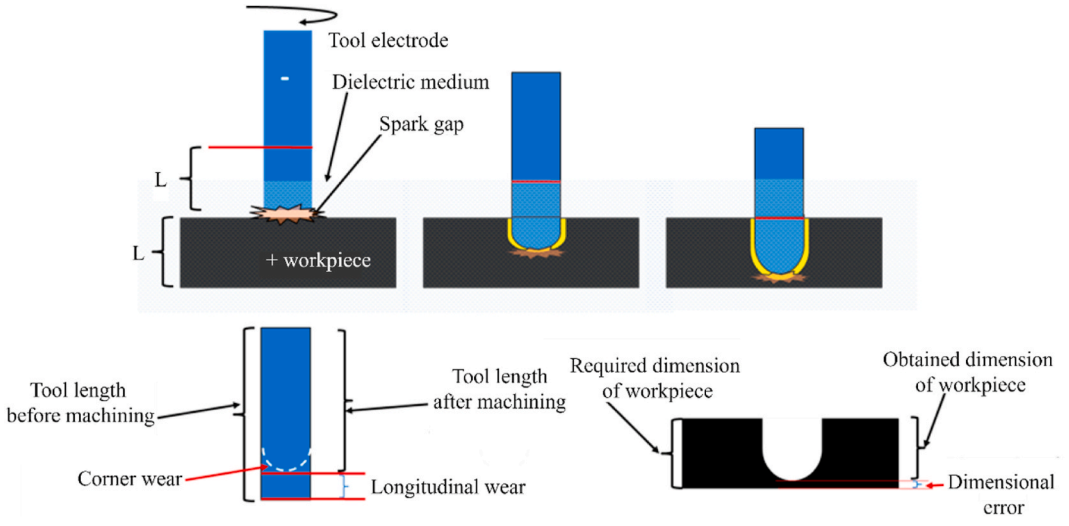

Fig. 1. Schematic diagram of dimensional inaccuracy caused by tool wear.

process is termed the formation of an ionization channel. Since the ionization channel produced is conductive, dielectric breakdown occurs, and thus a discharge is generated. The heat energy is generated by converting the kinetic energy of ions and electrons at the anode and cathode. Localized melting and evaporation of the electrodes occur due to the heat produced by discharge canals, which can generate up to 1017 W/m^2.

Consequently, the tool erodes as the machining progresses, making it necessary to estimate the volumetric wear ratio, which commonly leads to inaccuracies in the size and shape of the components [14]. Multiple pulse generators facilitate ongoing sparking and enable the machining process to proceed. These encompass servo feed controllers, transistor-based systems, and pulse generators utilizing RC discharge circuits. Moreover, combinations of different generators to increase the machining efficiency of μEDM were reported in the literature. A conventional RC-type pulse generator has a material removal rate that is 24 times slower than a combination of a transistor-type pulse generator and a servo feed controller [15]. μEDM drilling has shown the capability to produce three-dimensional micro holes [16], micro rods with a diameter of 60 μ m [17], and micro-holes less than 5 μ m in diameter [18], among the various micromachining techniques. These features are generated by various micro-EDM alternatives, classified according to electrode traversal or the polarity of the specimen and electrode. Material removal in μEDM is subject to contributing and non-contributing types of discharge pulses, which are dissimilar in frequencies, dimensions, profiles, and discharge durations. These discharge pulses are influenced by capacitance, material properties, voltage, and dielectric properties [19]. During flushing, there is considerable unpredictability in the size and shape of the pulses, electrode, specimen orientation, tool polarity, and workpiece. This uncertainty in pulses leads to irregular discharge energy and undesirable short circuits. This ultimately results in relatively high tool wear, which is undesirable during machining; thereby, the dimensional accuracy of the fabricated components is critically affected. A schematic diagram illustrating how tool wear affects the accuracy of manufactured parts and electrodes is shown in Fig. 1. Dimensional inaccuracies caused by tool wear in μEDM-manufactured micro-holes with dimensions greater than 5 μm cannot be ignored [20]. Tool wear damages the accuracy of various features and affects the machining performance; hence, tool replacement becomes essential. The tool wear issue becomes more significant in the μEDM process as the minor defects in the electrode contribute significant errors to micron-scale features. Therefore, it is essential to have a mechanism capable of monitoring and compensating for such electrode wear during the μEDM machining process.

The discussion shows that tool wear significantly influences the precision of the products fabricated by μEDM [21,22]. The following section highlights the different types of tool wear and their progress. Various researchers have made numerous attempts to address this tool wear problem. Some of the proposed efforts have highlighted the benefits and drawbacks of μEDM. However, substantial challenges persist, including effectively monitoring electrode wear and ensuring the applicability and validity of proposed compensation methods across a range of input parameters and materials. This systematic review aims to link with a proposed future research plan for more effective electrode wear compensation in real-time.

2. Tool wear in μEDM variants

2.1. *μEDM drilling*

Tool wear is intrinsically related to the μEDM procedure and is usually produced by unsteady discharges during machining. With increased drilling depth, the flushing pressure required to remove debris becomes insufficient and causes secondary discharge. Secondary discharges result in tool wear at the edges and tips of the electrode, leading to depth inaccuracies and taper growth in micro-hole sidewalls. The cross-section of a microscopic hole produced by μEDM, aimed at a depth of 600 μ m, is depicted in Fig. 2 (a) along

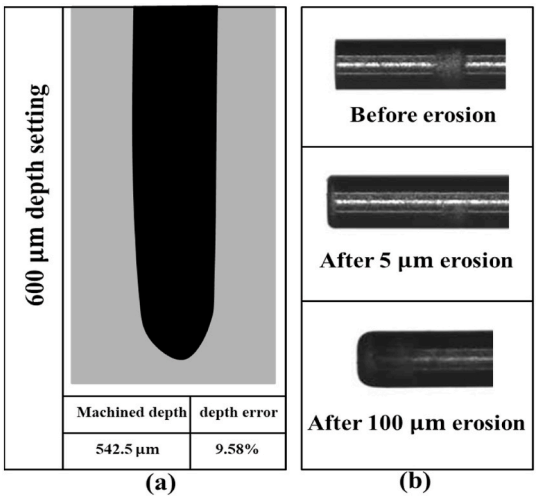

Fig. 2. (a) depicts the discrepancy in the intended depth of micro-holes due to electrode wear [23], while (b) shows the tool wear after machining specific depths [21].

with tool wear at different depths, as shown in Fig. 2 (b). However, it was revealed that the machining depth was only 542.5 μ m (i.e., 9.58% error) [23]. The required depth set on the CNC control panel of the machine was 600 μ m. Even after machining, the CNC controller indicated that the depth in the Z-axis had been achieved (i.e., 600 μm). Kurafuji and Masuzawa [24] introduced the first scaled-down version of EDM in 1968 and noticed a dimensional precision error of 10% in the holes due to electrode wear. Since then, several researchers have explored various materials' electrode wear rates (EWR) across different parameter settings. Yu et al. [25] investigated tool wear during the μEDM process for three-dimensional cavities, noting substantial wear when removing a 30 μm thin layer. Mohri et al. [26] analyzed tool wear in EDM and proposed that a carbon film settled on the cathode and anode significantly influences MRR and minimizes the EWR. Jeong and Min [27] proposed a statistical simulation design of μEDM drilling with a spherical tool to determine the shapes of the electrode and a drilled cavity. The proposed model can precisely determine the variation in the electrode and specimen shapes during the machining process because of corner wear, as depicted in Fig. 3. The predicted error amounts to 13% when compared to the experimental outcome.

Pham et al. [28] conducted a study on the application of EDM for drilling micro-tubes and micro-rods. They delved into the effects of different variables on micro-tool wear in this process. The author employed a straightforward approach to calculate the volumetric wear ratio by utilizing the acquired geometric data. Fig. 4 depicts the size and shape of the hole created during the steel drilling with a WC (tungsten carbide) tool under specific sparking conditions.

Kurnia et al. [29] implemented an improved theoretical design and presented an analytical study of μEDM performance measures through crater volume prediction. They discovered that analytically derived responses, such as Material Removal Rate (MRR) and EWR, exhibited a 30–40% disparity compared to their corresponding experimental data. Fig. 5 depicts the development of wear on the tool at various depth settings.

Jahan et al. [30] proposed different electrode wear and tool dressing strategies while machining a 300 μ m diameter hole with the WC electrode. A uniform wear ratio for μEDM of WC was found to remove material from 70 to 80% at high current and voltage configurations. The various stages involved in maintaining the geometric accuracy of the tool for micro-hole machining are illustrated in Fig. 6 (a - c).

Fu et al. [31] conducted a study to investigate how the side gap width, EWR, and dielectric fluid influence the quality of rough, semi-finished, and finished surfaces. It has been found that the width of the surface edge gap increases as the machining power and feed rate increase. However, the EWR increased with the machining feed rate, and it has been reported that the EWR of WC was always higher than that of the tungsten tool. Fig. 7 (a, b) depicts the detailed outline of the tool before and after machining in water whereas Fig. 7 (c, d) represent the same for oil.

Hourmand et al. [32] introduced a novel approach for manufacturing and measuring microelectrodes characterized by a high aspect ratio. This method incorporates an innovative problem-solving technique. The tapered and nonspherical micro-tool, manufactured by employing the standard electrode (circular type), can be seen in Fig. 8(a) and (b). Following their investigation, they successfully fabricated a micro-hole with an impressive aspect ratio of 60.25. This micro-hole, which measured 4.70 mm in length and 78.19 μm in diameter, was achieved by initially creating a through-hole (134.5 μm in diameter) on WC-Co.

Kumar and Singh [33] conducted a study to examine the impact of characterized micro-holes at two distinct angles of inclination, specifically between 60° and 70° from the horizontal. The author explored variations in hole width and electrode speed to amplify the output characteristics. By utilizing a specialized tool intended for cutting 0.8 μm-wide holes, a noteworthy enhancement in aspect ratio by 300% has been proposed in contrast to a solid spherical tool. Fig. 9 (a, b) presents the schematic of the tool electrode with multiple slots. Fig. 9 (c) visually compares the electrodes before and after the machining procedure.

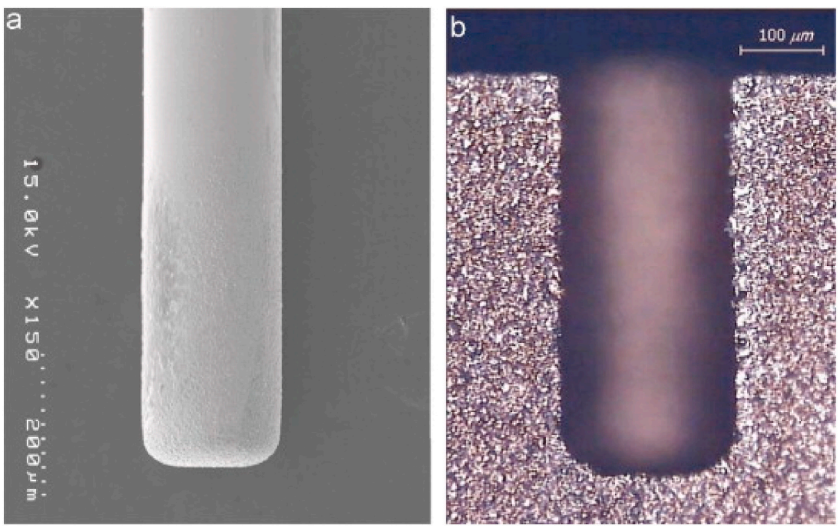

Fig. 3. Scanning electron microscopy (SEM) image of electrode and workpiece when the drilling depth is 580 μm: (a) tool and (b) workpiece [27].

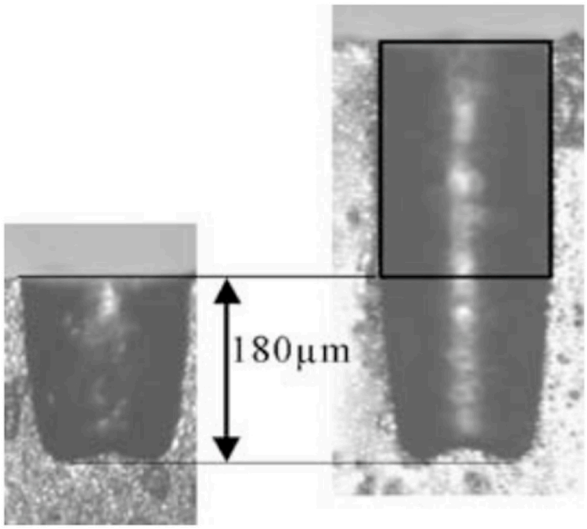

Fig. 4. Constant tool shape into the workpiece after a 180 μ m erosion depth [28].

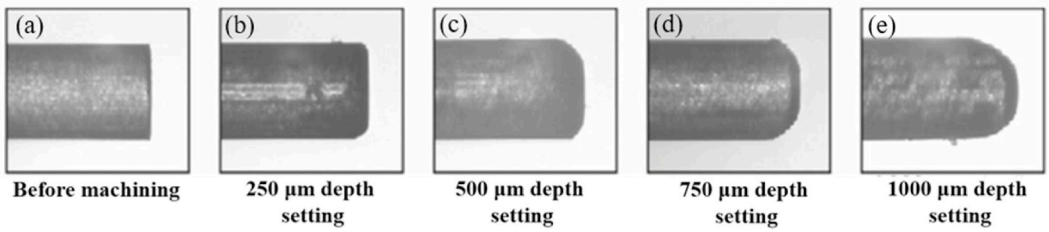

Fig. 5. Electrode wears for depth settings of (a) before machining, (b) 250 µm, (c) 500 µm, (d) 750 µm and (e) 1000 µm [29].

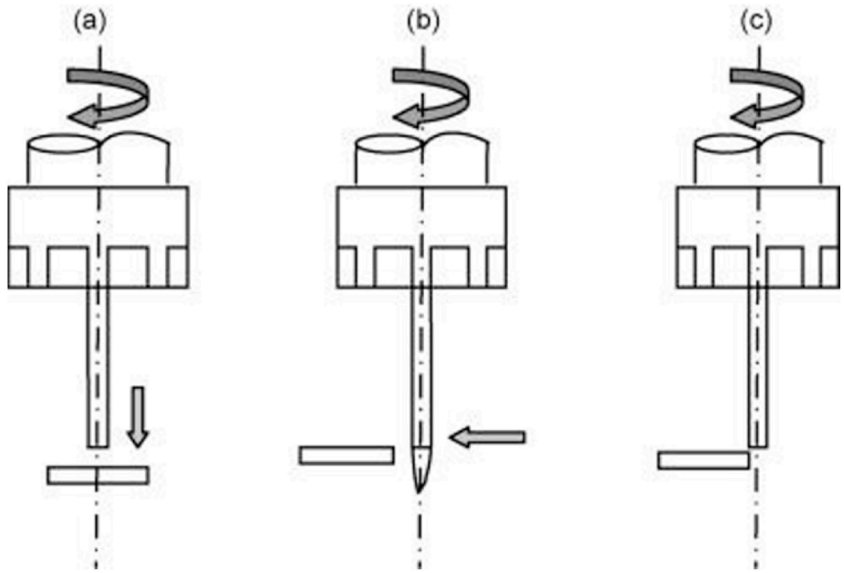

Fig. 6. Electrode dressing for the micro-EDM of micro-holes: (a) drilling of micro-hole by micro-EDM, (b) dressing the taper length horizontally, and (c) approaching the next hole [30].

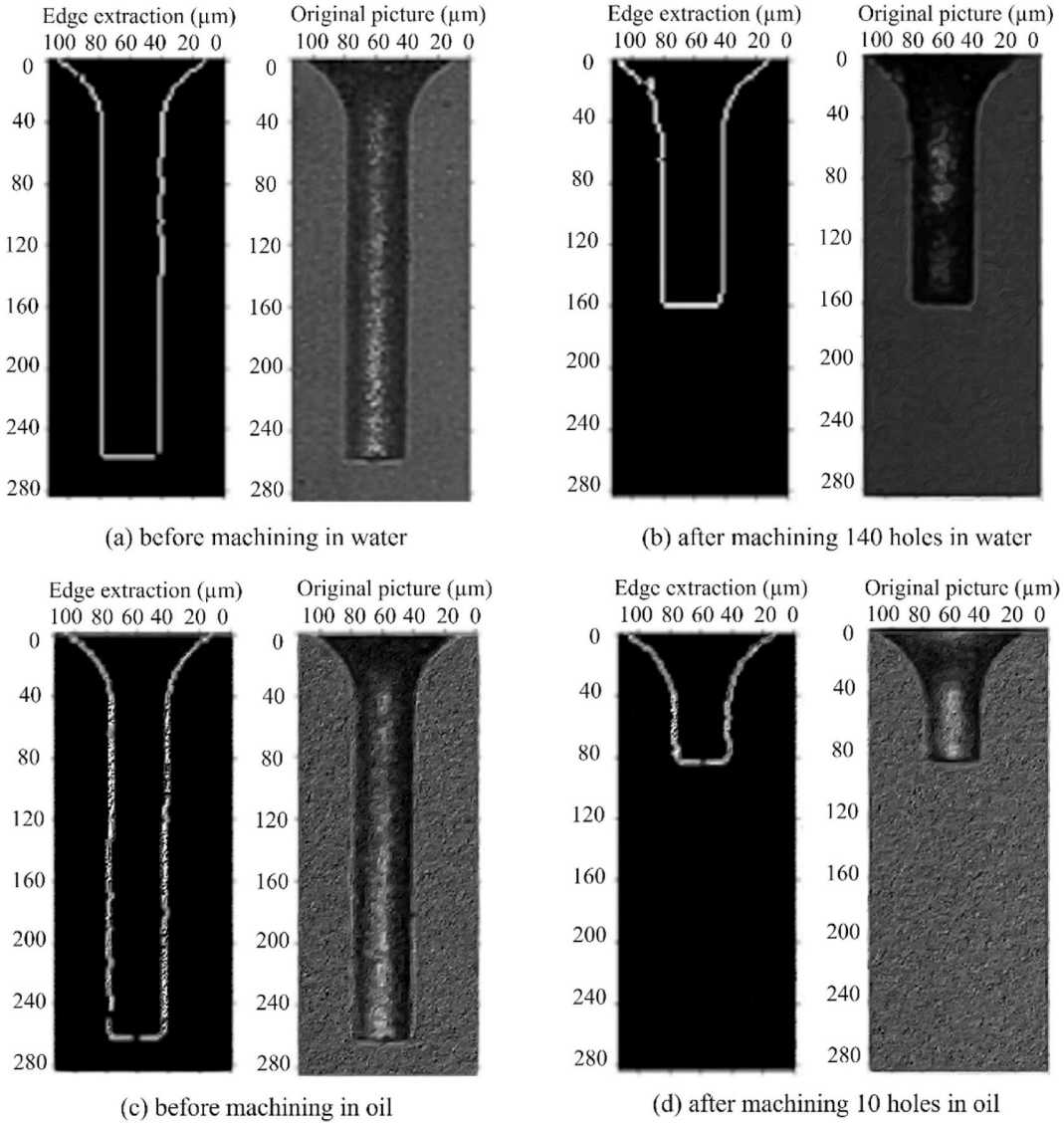

Fig. 7. Alteration in the appearance of tungsten electrodes (a) before machining in water, (b) after machining 140 holes in water, (c) before machining in oil and (d) after machining 10 holes in oil [31].

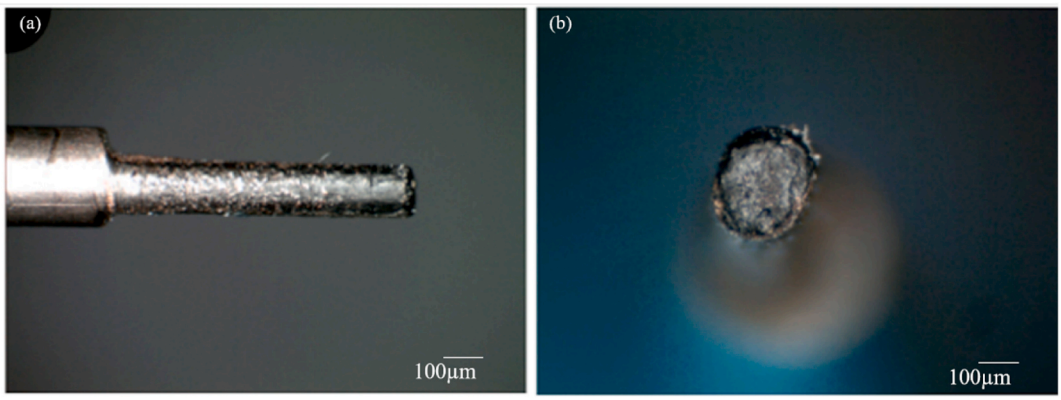

Fig. 8. Taper and non-cylindrical microelectrode with (a) front and (b) side views [32].

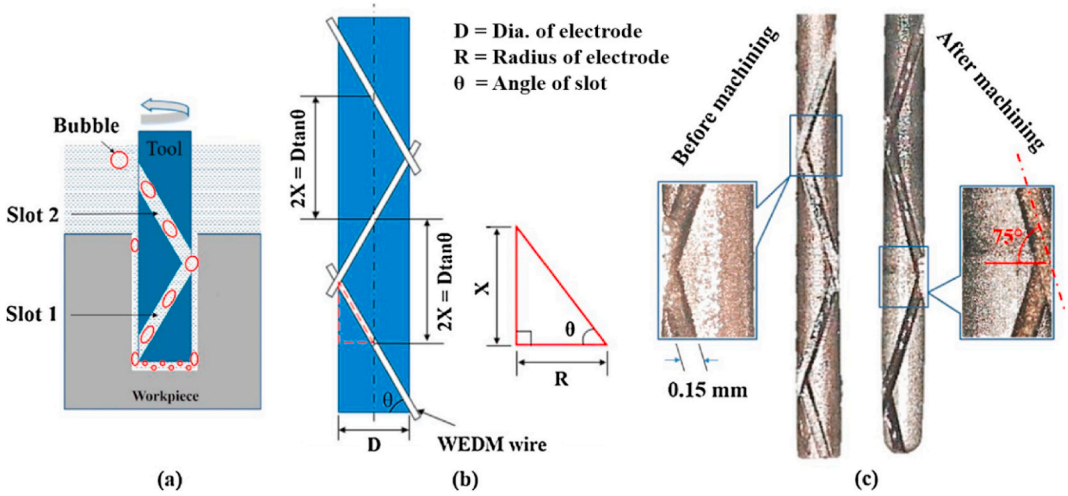

Fig. 9. Schematic of the tool electrode with multiple slots (a, b), (c) actual electrode [33].

2.2. *μEDM milling*

As micro-EDM drilling operates in a two-dimensional manner, several researchers have explored three-dimensional milling techniques to overcome the limitations inherent in this machining method. The EDM method is subdivided into two alternative processes for making micro-molds. The standard type in EDM is die-sinking; however, it has several drawbacks. One of the drawbacks is the requirement to fabricate a multi-shape tool before the removal process, which is expected to be expensive and complex. A contemporary manufacturing machining method that also depends upon the spark for material removal is the μEDM milling process. This machining method uses a circular tool to create a defined shape by retrieving the computer numerical control (CNC) code. These codes encompass the electrode path for layer-by-layer micro-EDM milling processes with a depth limit typically around 0.1 μm per layer. This machining method must use a stipulated wear compensation approach to remove electrode wear, which is crucial for the manufacturing accuracy of three-dimensional geometries.

In the nineties, μEDM milling was developed in Charmilles for spherical tools with diameters ranging from 0.8 to 12 mm. Mehfuz and Ali [34] formulated a numerical model that employed comprehensive three-phase factorial experimental designs to investigate how capacitance, feed rate, and voltage influence the outcomes of the machining process. They achieved an optimization level of 88% desirability by determining the optimal surface roughness (SR) values at 0.04 μm, EWR at 0.044, and MRR at 0.08 mg.min-1. Heo et al. [35] suggested a 3D geometric analysis technique for μEDM milling. A 'Z' map algorithm was also developed by Mehfuz and Ali [34] to obtain precise information about variations in the tool's geometry and the workpiece due to electrode wear during machining and also investigated the influence of machining parameters on the outcomes. Bissacco et al. [36] employed a laser scan micrometer within a manufacturing setup to investigate tool wear in μEDM milling. They determined the coordinates of a tooltip before and after the machining process. Karthikeyan et al. [37] conducted a comparison of various μEDM milling techniques, considering channel geometry and SR of the machined workpieces. Their findings propose that the tool's surface remains unaltered by centrifugal force during

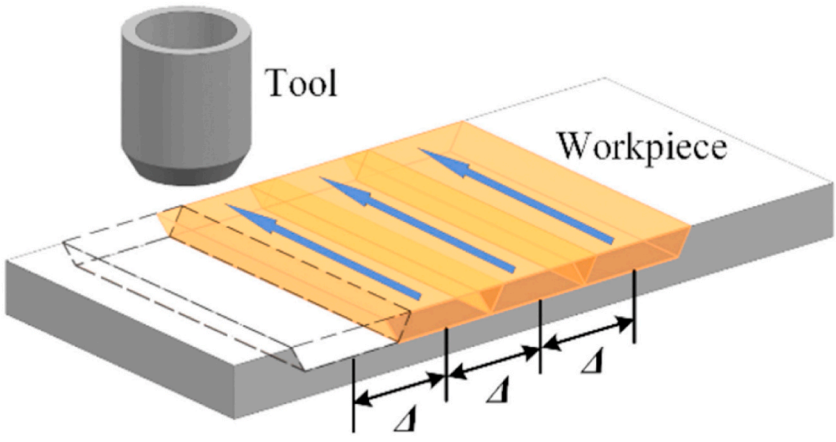

Fig. 10. Schematic diagram of flat milling using a cylindrical tool [40].

the machining process. Since tool wear influences the precision of the machined surface, various methods have been adapted to judge and compensate for electrode wear. Wei et al. [38] introduced an innovative assessment approach to improve μEDM milling performance, particularly for challenging-to-machine materials. Their method demonstrated a remarkable 30% improvement in manufacturing hard-to-machine material. Nguyen et al. [39] presented a geometric model to simulate the effects of three-dimensional μEDM milling on the machining mechanism. The corner radius of the plain electrode, electrode wear, and IEG influenced the precision of machining. Pie et al. [40] offered a flat milling procedure based on the constant length compensation approach. This investigation addresses the constraints of the previously studied constant tool length compensation strategy. Fig. 10 depicts a conceptual diagram of the flat milling procedure using a cylindrical tool. Fig. 11 (a - e) presents the shapes of tool with different milling distances. It illustrates that the flat base at the end of the reduced conical tool, as opposed to the conical tooltip, permits plane milling without extra precautions.

2.3. Reverse μEDM

Reverse μEDM (RμEDM) is identified as the most advanced method in the μEDM field. This technique has been employed to produce high aspect ratio micro-features with diverse applications in micro-EDM, encompassing the drilling of cavities in fuel injection nozzles, turbine blades, and spinners. Productivity can be enhanced with the help of such selected micro features. The RμEDM procedure is carried out in two steps. During the initial phase, appropriately sized holes are machined on the tool plate using the micromachining process. In the next phase, RμEDM is used to replicate similar holes. Yamazaki et al. [41] proposed the fabrication of micro rods using a technique wherein a pre-drilled micro hole plate served as the tool plate, and the polarity of micro-EDM drilling was inverted. Fig. 12 (a–c) depicts a detailed view of micro rods after the machining at different discharge powers. Under conditions of equivalent electrical capacitance, the smallest difference between the voltage and IEG likely caused the tool's diameter to grow while the voltage decreased.

Kim et al. [42] forwarded the investigation and named it RμEDM. This technique successfully manufactured micro rods smaller than 30 μm in diameter on tungsten carbide (WC) material. The tool wear in RμEDM is shown in Fig. 13 (a, b) and fabricated micro rods are depicted in Fig. 13 (c).

Since the development of RμEDM, researchers have individually explored diverse combinations of workpieces and electrode materials to ascertain their viability for producing specific microrods [43–45]. Hwang et al. [43] utilized vibration-supported mechanical peck drilling and RμEDM techniques to produce a micro pin array measuring 40 × 40 μ m on WC material. Yi et al. [44] achieved the successful fabrication of an array of copper tools measuring 3 × 3 μm and 4 × 4 μm by utilizing a tool plate composed of 100 μm thick AISI 304 stainless steel. The electrode plate perforations were made by μEDM drilling with a single 80 × 80 μm tool having a rectangular region, as shown in Fig. 14 (a, b). Such selected micro tools were then employed to manufacture the pattern of 3× 3 μm and 4× 4 μm holes on metal foils through batch model μEDM drilling, as depicted in Fig. 14 (c, d). They also concluded that by employing batch type μEDM drilling, the production was enhanced up to four times compared to a single tool.

Zeng et al. [45] used ultrasonic vibrations in the tool plate to improve the machining efficiency of RμEDM. A reduction in machining time of up to 2.5 times was observed by authors when using ultrasonic vibration. Hwang et al. [43] also established new dielectric flushing methods to improve machining performance in ultrasonic vibration. Several researchers have attempted to understand the process of the RμEDM method and conducted parametric studies on the quality of manufactured micro-rods [44–46]. Mastud et al. [46] compared μEDM drilling and the RμEDM based on current and voltage signals, reporting that the overall stability of RμEDM technology was more outstanding compared to μEDM drilling due to a longer standard discharge time. They also proposed that the RμEDM method can be operated at the maximum capacitance and voltage range without significantly increasing arcing. Debris deposition on the face of micro rods tends to result in insignificantly higher SR than the hole machined by μEDM drilling. Majumdar et al. [47] determined the impact of threshold, voltage, SR, capacitance, and dimensional accuracy of RμEDM on brass material, revealing that the dimensional imprecision involves differences in the diameter and length of the micro-tools. The presence of secondary discharges reduces diameter inaccuracies at the tip of the micro pin while increasing inaccuracies at the base. Mastud et al. [48] studied the effect of dimensional accuracy and electrode plate thickness on the volumetric EWR. They suggested that optimal heat transfer led to a reduction in electrode wear for the thick tool plate. Such elevated electrode wear fractions can introduce a large dimensional error in the manufactured parts. Therefore, tool wear compensation is provided to remove these errors and reduce EWR. A brief summary of tool wear in different μEDM operations is presented in Table 2.

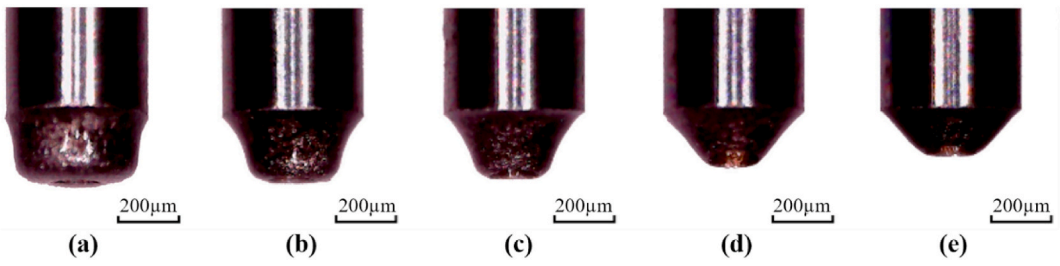

Fig. 11. Shapes of the tool with different milling distances at (a) 200 μm, (b) 600 μm, (c) 900 μm, (d) 1200 μm and (e) 1500 μm [40].

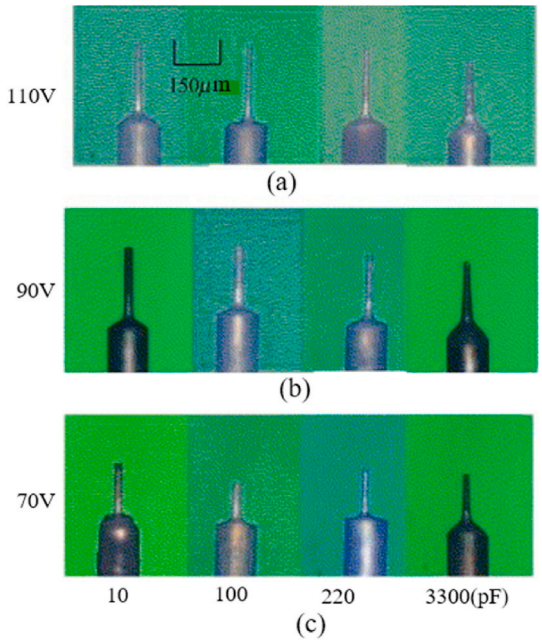

Fig. 12. A photographic view of electrodes obtained by altering discharge energy through (a) 110V, (b) 90V and (c) 70V [41].

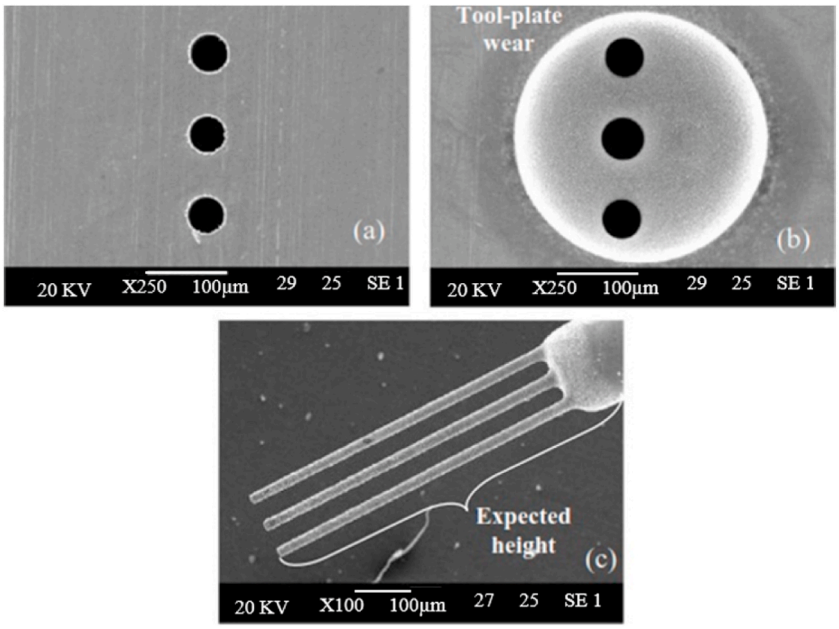

Fig. 13. Tool plate consisting of the micro-holes (a) prior to machining, (b) post-machining, and (c) a combination of micro-rods that have been manufactured [42].

3. Tool wear compensation (TWC) techniques

Tool wear during machining is inevitable, and the deterioration of electrode shape can directly impact the depth and profile of microstructures. The electrode shape changes quickly when milling or drilling μEDM with a micro-spherical tool. These changes in the electrode increase the wear on either end of the electrode or the side face (circumference), signified as corner and front wear, consistently. Front wear of the tool during μEDM causes an error in the tool length, which is mainly responsible for the inadequate micro-hole drilling depth. Corner wear of the μEDM milling tool leads to rounded electrode edges and impairs the microstructure's geometric precision. There is significant potential to address these electrode wear issues and develop techniques to enhance the

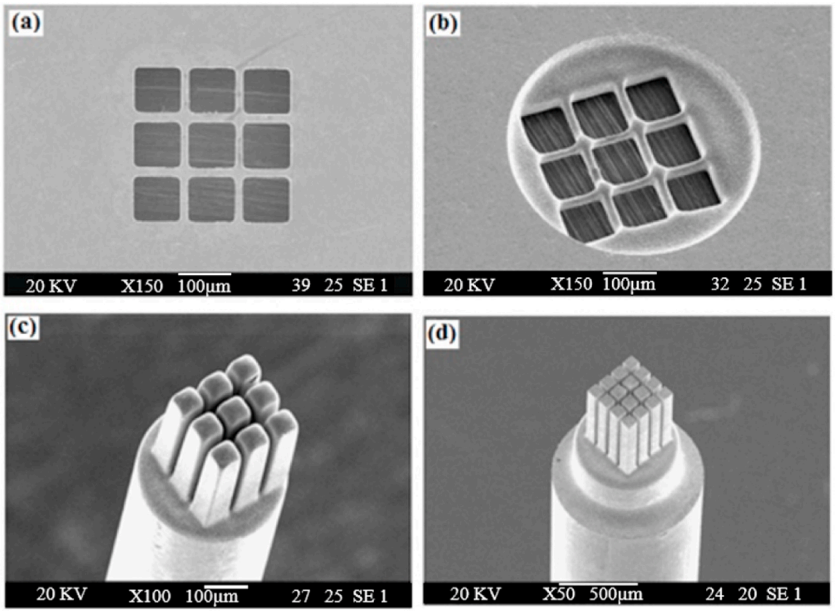

Fig. 14. A 3 × 3 negative-type electrode arrays fabricated by micro-EDM using a single electrode: (a) before use, (b) after use, and an array of Cu electrodes fabricated by REDM with 80 × 80 μm square cross-section: (c) a 3 × 3 array after use, (d) a 4 × 4 array before use [44].

Table 2
Tool wear in μEDM.

	μEDM Operations	Description
Tool wear in μEDM	μEDM drilling	Data-driven regression models have been successfully used for measuring the tool wear rates in μEDM drilling. Tool wear in μEDM drilling is significantly affected by open voltage.
	μEDM milling	In μEDM milling, tool wear refers to the gradual deterioration or erosion of the machining tool's cutting surface due to repeated electrical discharges, impacting machining accuracy and quality over time.
	Reverse μEDM	Using this technique, high aspect ratio micro-features have been produced using a variety of micro-EDM applications, including the drilling of cavities in fuel injection nozzles, turbine blades, and spinners with minimum tool wear.

machining precision using electrode wear compensation for μEDM. A tool wear compensation (TWC) technique in μEDM was proposed by Yan et al. [49] by employing visual measurement of the electrode. Under constant feed rate during machining, the extent of front tool wear correlates with the depth of grooves and holes. When working with predetermined grooves and hole depths, increasing the machining feed rate enhances the length of front wear. The increase in machining depth leads to the expansion of the discharge region at the electrode's edge, resulting in a sharper electrode known as corner wear, as illustrated in Fig. 15 (a, b).

However, in the past 7–8 years, several attempts have been made to solve the electrode wear problem only in μEDM milling. In μEDM, compensation methods are applied either offline or online to resolve the issue of tool wear, and thus, they are named offline and online compensation techniques. The results of tool wear issues in μEDM were mainly attempted through offline compensation, and after that, some efforts were made by using the online compensation method as well. Both offline and online compensation methods

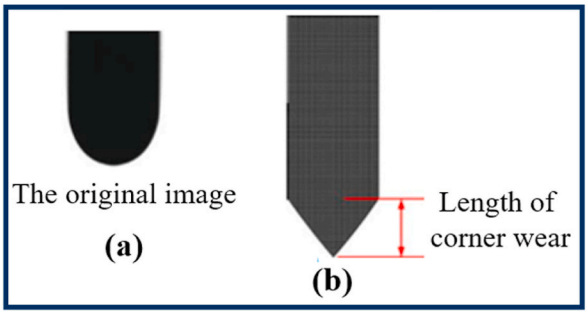

Fig. 15. The geometry of (a) the actual image of the electrode and (b) the measurement of corner wear [49].

are discussed in different sections. A brief summary of tool wear compensation techniques in μEDM operations is presented in Table 3.

3.1. Offline compensation techniques

The offline tool wear compensation procedure primarily involves assessing tool wear through EWR, often calculated during testing at periodic intervals throughout the machining process or at the start. Since the 1980s, tool wear has been determined regularly with the help of different tool wear sensing approaches such as laser sensors, machine revelation methods, etc. [50,51]. The actual execution of the downward exertion is an effective compensation determined by the model of offline electrode wear before machining. Despite applying analogous solutions in diverse manufacturing contexts, these solutions have not yet emerged as pioneering trends in tool wear compensation. The offline compensation technique determines the required electrode length reduction for each tool path segment. During this calibration process, the material removal from the workpiece is compared to the wear in volume that is proportional to it.

3.1.1. Periodical enhancement of tool wear compensation

A comprehensive analysis of electrode length can be used to provide expected compensation and minimize tool wear during machining. Accurate electrode length determination permits the precise verification of actual electrode wear. Following each layer, calculations for electrode length and anticipated wear compensation are generally performed due to the iterative nature of machining in consecutive layers. The tool wear compensation algorithm relies on the average of the sample depth and layer width error. Using offline wear compensation based on relative volumetric wear and machining, an adequate number of layer depth inaccuracies was minimized to 5 μ m [52]. Significant compensation must be made for tool wear to obtain the required precision in produced components. Machine vision, uniform wear methods (UWM), and linear compensation (LCM) are popular electrode wear monitoring and compensation techniques. The arrival of the machine vision method made the tool and workpiece image analysis faster, more flexible, cheaper, and easier for automation. This is a non-contact type measurement method and, therefore, appropriate to measure an area from the surface of the work material compared to a single line. The UWM integrates a tool path algorithm with longitudinal tool wear adjustment, resulting in a notable enhancement in the accuracy of EDM milling. The UWM technique utilizes counter-machining, having the minimum possible feed per layer, and exclusively employs the bottom of the electrode for manufacturing. The TWC has been implemented in LCM by feeding it into the specimen for a specific duration as it travels along the tool path. In the traversal space, the tool feed depth must be kept fixed. Such a method only guarantees electrode end wear and is ineffective in machining the three-dimensional composite profile [25].

3.1.2. Machine vision measurement method

In the machine vision measurement method, firstly, compressed air is used to blow off the dielectric liquid droplets from the electrode. After that, the tool was dragged to where the machine vision process would be operated. The tool's shadow reflection and deformation are obtained using an equivalent light source. This technique may be more effective for determining drilling depth in specimens since the tool's surface color is darker than the algorithm for light processing detection lines. This algorithm determines the drilling depth by using a drop of dielectric fluid to measure the tool length and rapidly and efficiently drill into the work material [50]. In 1989, Kaneko et al. [50] employed the layer-by-layer EDM method and suggested an electrode wear compensation method of a rotating axisymmetric electrode. The compensation arrays were measured experimentally. Electrode wear was expected, and the electrode path was automatically selected to compensate for the wear. Kaneko [53] adapted the tool wear compensation technique in 1992 by adding a charge-coupled device (CCD) camera to the EDM testing machine to capture the electrode's profile. Fig. 16 (a) depicts the experimental setup and Fig. 16 (b) represents the captured electrode image.

Kim et al. [54] subsequently created a machine vision system comprising a CCD camera and specialized jig to ascertain the extent of electrode wear. Guo et al. [55] suggested a tool wear adjustment based on the machine vision method for manufacturing micro tools. As discovered by the study, a comparison of the SEM findings with the tool diameter array yielded a 3% discrepancy. Dong et al. [56] used a CCD camera during the investigation and proposed high performance for creating micro-holes with a high aspect ratio (HAR). They found that the taper angle and tool wear diameter increased as the current rose. However, machining constancy decreased when the current reached 3.5A. The study demonstrated that machining micro-holes with a high aspect ratio is not ideal when utilizing high currents. The detailed view of the experimental setup with a visual optimization arrangement is depicted in Fig. 17.

Sortino [57] provided an electrode condition monitoring system that can be used to identify the worn-out region of the electrode. Various systems, such as infiltration and high pass, were employed to determine the surface shape and remove the material. The author observed that even little changes in the amount of material removed from the workpiece were associated with large shifts in the measured inaccuracy. To ascertain and control the size of a thin tool during μEDM, Lim et al. [58] developed a visual sensor. The

Table 3
Tool wear compensation techniques.

	Types	Description
Tool wear compensation techniques.	Offline compensation	The offline compensation approach is used when an anticipated tool wear compensation is added at the start of the machining or at regular intervals to reduce the machining error.
	Online compensation	Online compensation is generally utilized for combining anticipated compensation with real-time compensation. It increases the scope for machining blanks for which the accurate shape is not determined.

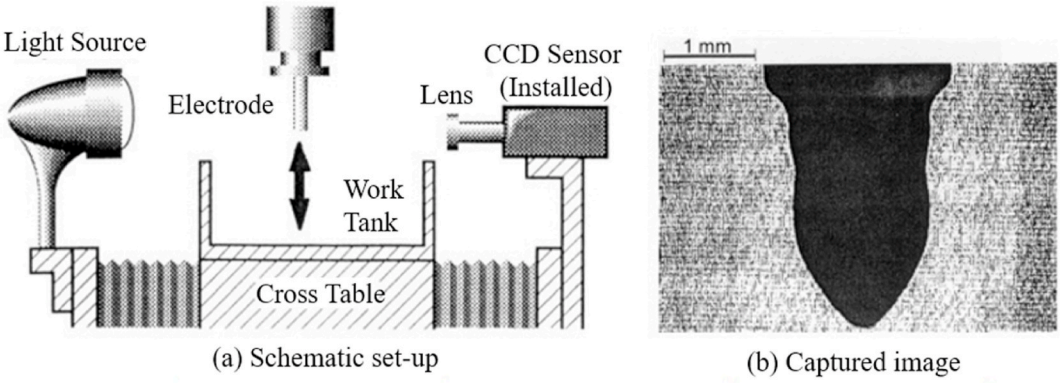

Fig. 16. Representation of the optical measurement method with (a) Schematic set-up and (b) Captured image [53].

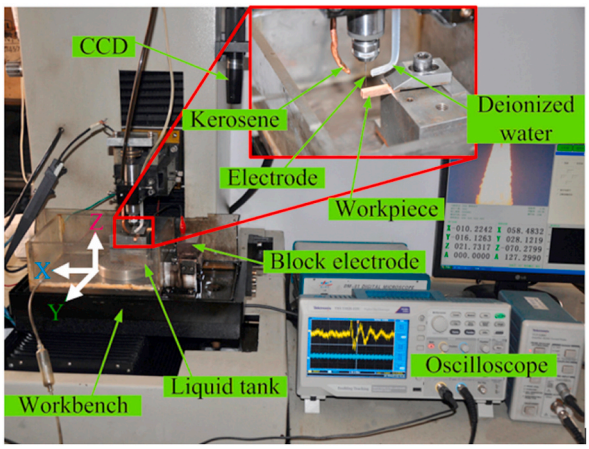

Fig. 17. A photographic view of the experimental setup [56].

measured depth of cut is inversely proportional to the turning tool's aspect ratio and feed rate, as discovered by the authors. Jurkovic et al. [59] employed a laser diode approach during the machining to detect the size and depth of the crater in the workpiece. They performed a significant surface analysis with the help of a three-dimensional image of relief during the machining. Huang [60] investigated developing the original measurement system by applying the machine vision method. The investigation result shows optimal precision and efficiency for measuring electrode length and drilling deepness under different conditions. Based on the crater

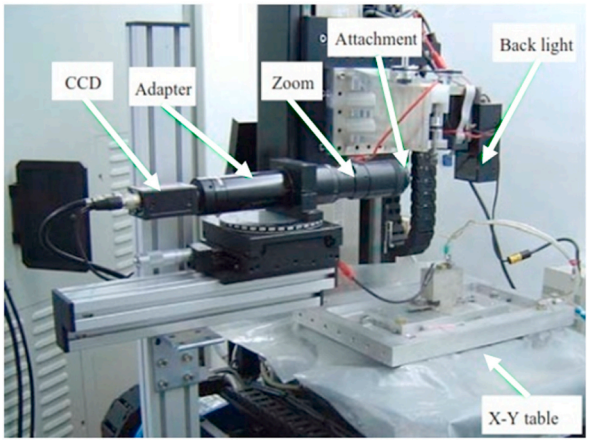

Fig. 18. Experimental configuration used to measure tool wear with a machine vision system directly [49].

calculation, Kurnia et al. [29] suggested an analytical study of the μEDM method. The analyzed responses of MRR and TWR were obtained with a difference of 30% and 24%, respectively, from the selected experimental values. A TWC for the EDM procedure was introduced by Yan et al. [49], utilizing the machine vision system. The electrode's front and corner wear were assessed and compared using machine vision image processing. The front wear span at a constant feed rate was observed to be linearly influenced by hole and groove depths. At a particular hole and groove depth, higher feed rates lead to a longer front wear length for the tool. A machine vision system for compensating tool wear is shown in Fig. 18, and it is important to note that production times may be extended by up to 40% when using UWM.

Yan et al. [61] introduced a novel 3D EDM multi-cut machining process and TWC technique using a machine vision approach. The inquiry's findings showed that the multi-cut development process and TWC approach could drastically improve the machining precision for the EDM process with reduced machining time. Moreover, with the micron system, X–Y dimensional inaccuracies can be limited to 10 μ m. One of the significant challenges in EDM-related work is predicting tool wear, as it can greatly affect the components' precision and the machining process's stability. Various attempts have been made to incorporate tool wear-induced volumetric errors using assessment or monitoring methods for achieving high-precision machining.

3.1.3. Linear compensation method (LCM)

The LCM is an existing method for assuring advanced machining electrode wear compensation in three-dimensional μEDM milling [25,62]. The conventional LCM approach relies on experimental models that must be adjusted and updated through offline tool wear compensation to account for a specific electrode wear behaviour. The LCM approach relies on a compensation parameter for electrode wear to ensure machining accuracy and compensate for wear along the electrode's length. LCM is a process that compensates for electrode wear with a continuous or slight increase in the electrode path. The authors in Refs. [60,62] reported that the electrode traversed downward in this method. After covering a certain distance, it was used to machine a 9×9 mm^2 hole by placing a 1 mm diameter electrode. The final smoothing below the hole was within 2 μm of the Ra value. However, the compensation measure in LCM is generally an experimental value that depends on extensive testing. This method only produces three-dimensional microscopic parts with straight sidewalls [63,64]. It is theoretically verified that the LCM is not suitable for making complex three-dimensional profiles using μEDM. A capable and efficient process for compensating electrode wear during high-accuracy EDM of complex 3D micro holes was proposed by Wang et al. [65], which involves in-situ pulse monitoring. The combined process's behaviour was influenced by a crucial parameter, namely the change in the tool path pattern.

Moreover, an 80% reduction was obtained from the original offline compensation method. Wang et al. [66] developed an in-situ method for measuring process dynamics and pulse performance under different electrode wear compensation conditions after investigating the LCM principles. Their findings indicated that a time-saving of 18% during the machining process was achieved by preserving the necessary dimensional and shape accuracy. Fig. 19(a–c) indicates that the hole depth may be shallower than the target depth due to average electrode wear compensation, but overcompensation can lead to a deeper hole cavity.

3.1.4. Uniform wear method (UWM)

To overcome the restrictions mentioned above of LCM, UWM was introduced. In the UWM, the entire machining process involves milling multiple thin layers simultaneously. Before generating a uniform layer, the electrode is consistently adjusted for each layer to maintain the desired machining depth. Yu et al. [25] developed a straightforward machining technique to address longitudinal tool wear in EDM milling. The to-and-fro scanning tool paths continually machine the border and internal section of the hole. After machining a layer, this technique can potentially restore the electrode profile to its initial dimensions. In addition, UWM already produces random three-dimensional micro holes with CAD/CAM [67]. Kruth et al. [68] used an offline compensation method to analyze the tool wear for each section in their proposed standard EWC method. This compensation depends on the offline measurement of actual volumetric wear and provides little inspiration for online wear compensation. Although EWR was extensively used in many offline TWC methods, many things could be improved in measuring EWR. Initially, the measurement of EWR was impacted by material and methodologies, but enhancements can be achieved by employing suitable geometries and increasing geometric time. In other words, the tool size was relatively small, resulting in a lower erosion rate from the tool compared to the working material. Therefore, the determination of EWR was influenced by high inaccuracy [64]. Nguyen et al. [40] also performed TWC using UWM, which gives a higher wear estimation than the theoretical model.

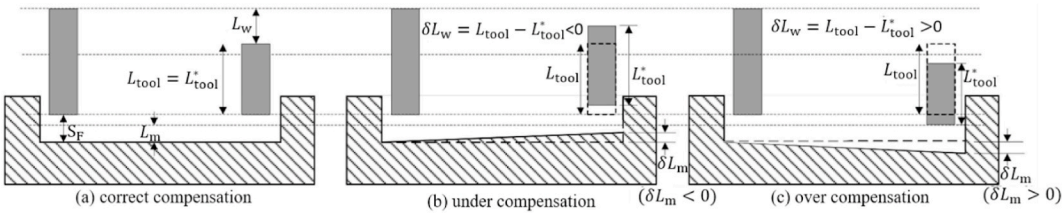

Fig. 19. Machining deepness error after a single machining layer owing to incorrect electrode wear compensating parameters with (a) correct compensation, (b) under compensation and (c) over compensation [66].

3.1.5. A combined linear uniform (CLU) method

Subsequently, the LCM and UWM were integrated to address the challenges posed by existing offline wear compensation methods. Upon amalgamating these processes, Yu et al. [22] referred to the combined approach as CLU. With this strategy, they improved machining and SR performance. The experiment illustrates that the proposed technique has enhanced machining response efficiency, with measurements such as MRR at 350 $\mu m^3/s$, EWR at 4–5%, and SR at 158 nm, as opposed to the performance of UWM. For the tool path design, CLU relies on UWM to ensure the varying size of the electrode tip after each machining layer. During the machining of each layer, the entire compensation length of the tool wear was distributed over several sections, and the whole tool path was covered. When a square hole was made on slanted planes, the maximum MRR with minimum TWR and SR was obtained compared to UWM [22]. In Fig. 20, the SEM image of the tool produced by the CLU process showed a flat tooltip, similar to the result of UWM. A theoretical framework was developed by Yeo et al. [20] to consider the influence of tool wear during the manufacturing of surface profiles. They found that experimental results closely matched the simulation. Machining using this model should have a precise surface profile, i.e., 0.14 mm for macro EDM and 1 μm for μEDM [63]. However, the model had the drawback of maintaining a constant cutting width. This limitation was addressed by reducing the tool path and specifying a single space between paths.

3.1.6. A fixed-length compensation method

Enhancing the performance of UWM and LCM requires increasing the thickness of the EDM milling layer. Pie et al. [69] proposed a fixed-length compensatory approach, which increases the probability of achieving a thicker layer thickness. They developed a very accurate theoretical model of electrode wear for the fixed-length compensation procedure. Precise theoretical models and substantial layer thickness correction achieved high accuracy and machining performance. Zhang et al. [70] employed a fixed-length compensation milling method to achieve a conic electrode end within a predetermined phase. As a result, additional steps must be taken to eliminate this variation, leading to a significant increase in the complexity of the machining process. The fixed-length compensation process necessitated electrode and work material sizes suitable for achieving a layer thickness below 85.5 μm. Using a spherical tool, Pie et al. [40] introduced an enhanced fix-length compensation approach for μEDM milling. The fixed-length compensation process was improved by replacing the cylindrical electrode with a tubular electrode. An analytical model was developed to account for the small conical profile of the fixed-length compensation factor. The study concluded that the manufacturing error was under 2%, and surface variation remained below 4 μ m for most conditions. Fig. 21(a–c) shows a schematic of a flat surface machined with a tubular and fluctuating surface machined with a cylindrical tool using fixed-length compensating μEDM.

By adapting conventional fixed-length compensation models, Zhang et al. [71] devised a multiple monolayer thickness milling process. They obtained advanced machining quality, accuracy, and performance of μEDM milling compared to the layer-by-layer conventional and UWM. The offline electrode wear compensation method involves temporary disturbance of machine functioning to measure tool wear directly. The tool was moved to a specific position where the compensation system could function appropriately. The periodic measurements of electrode wear and machining proved to be a very time-consuming process. The drawbacks of such compensation methods were removed by providing an online electrode wear compensation method. A brief summary of offline compensation methods in μEDM operations is presented in Table 4.

4. Online tool wear compensation

The compensation methods discussed in the preceding sections might not be optimal for addressing electrode wear compensation due to their disruptive nature, leading to prolonged machining periods. To surpass the constraints of the offline TWC technique an innovative real-time EWC technique has been introduced to eliminate dimensional inaccuracies. This particular compensation method is implemented in real-time throughout the machining to estimate electrode wear by recording data. The movement of an electrode and its compensation with the required path also depends upon the data received. This real-time compensation method can eliminate errors produced during the re-instalment of work material and electrodes [72]. The process is mainly driven by volume removed per

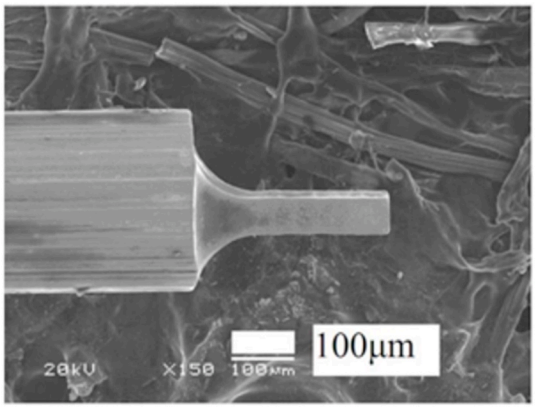

Fig. 20. Tool after machining with CLU [25].

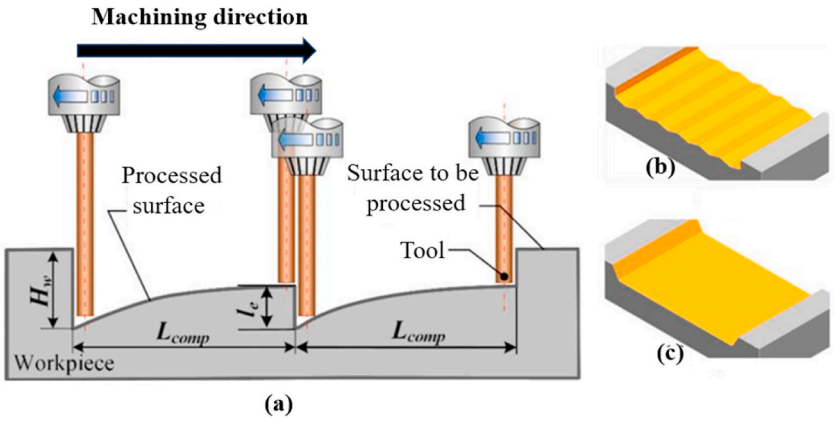

Fig. 21. (a) EDM fix length compensation schematic, (b) fluctuating surface machined with cylindrical tool, (c) flat surface machined by tubular tube [40].

Table 4
Offline compensation methods.

	Methods	Description
Offline compensation methods	Periodical enhancement of tool wear compensation	
	Machine vision measurement	Since the tool's surface color is darker than the algorithm for light-processing detection lines, machine vision techniques are useful for determining drilling depth in specimens. This technique quickly and effectively measures the tool length while drilling into the work material while measuring the drilling depth using a drop of dielectric fluid.
	Linear compensation method	The linear compensation method uses a compensation parameter for electrode wear to ensure machining accuracy and account for wear along the electrode's length. The compensation for electrode wear is carried out through a continuous or slight increase in the electrode path.
	Uniform wear method	In the uniform wear method, the entire machining procedure entails milling several thin layers at once. The electrode is continually adjusted before forming a homogeneous layer to maintain the appropriate machining depth between layers.
	A combined linear uniform method	This method combines linear compensation and uniform wear methods to deal with the challenges of offline wear compensation methods. Experimental evidence shows that this combined approach enhances machining response efficiency by 4–5%.
	Fixed-length compensation method	This method helps increase the milling layer's thickness, ultimately improving machining performance. This method replaces the cylindrical electrode with a tubular electrode.

discharge (VRD) from tool or work material. Real-time electrode wear compensation is a method that predicts and compensates for the real-time volume of material (V_{RT}) removed from the tool or workpiece during the machining process. Earlier, tool wear compensation relied on counting discharge pulses and applying a constant VRD value for determining the real-time amount of removed material from the tool and workpiece. It is crucial to accurately estimate the VRD because the VRD approach primarily depends on the tool or the workpiece. This can be accomplished through either the counting of discharge pulses or through the statistical pulse discrimination method. For electrode wear correction, the initial method entails multiplying the measured VRD by the count of discharge pulses registered from the tool or workpiece. The latter first discriminates discharge pulses into contributing and non-contributing ones and then considers only those pulses for such multiplication, contributing to material removal. Both types of online tool wear compensation methods are further explained separately.

4.1. Pulse counting based method

The online wear compensation method was devised to reduce the offline time required for determining TWC. This method indirectly counts the number of pulses (without interrupting the machine) while machining. This method compensates for the loss of fluorescence volume from the electrode or workpiece by measuring discharges with a pulse counter. The compensation can be performed using the pre-set electrode wear value per discharge and on the VRD. In 2002, Bleys et al. [73] first proposed a real-time TWC method for conventional EDM milling. They demonstrated a connection between electrode wear and normal discharges, assuming the pulses were isoenergetic. However, this approach cannot be used for μEDM because the pulses in μEDM are non-isoenergetic. Therefore, in 2004, Bleys et al. [74] presented a compensation technique that utilizes real-time electrode wear sensing and can address undesired profiles. The downward motion was predetermined according to the prescribed EWR, and the error caused by longitudinal electrode wear was removed.

Bhattacharyya et al. [75] proposed a method for monitoring electrode wear in complex and unpredictable surface milling

operations using continuous online monitoring. Liao et al. [76] categorized the RC power source pulses into different types, i.e., normal pulses, effective pulses, arcing pulses, temporary short, and complex pulses. They revealed that 60% of contributing pulses were obtained as a normal type with a small amount of effective and complex pulses during the low feed rate machining. In high feed rate machining, there is a low occurrence of normal pulses and a high occurrence of complex pulses. The pulse counting approach gives a significant dimensional precision of traditional display indicators of the μEDM machine system [77]. The accuracy of the method is based on analyzing small volumes and pulse counting, which are very stimulating. Yeo et al. [78] and Aligiri et al. [23] studied the real-time measurement of the MRR volume during single spark μEDM drilling. They revealed that the VRD undergoes significant changes when determining the different machining depths. This phenomenon was attributed to the formation of a substantial localized debris area and the enhanced control of debris overlapping as the machining depth increased. The author managed to drill a 900 μm hole with a minimal error of only 4%. Fig. 22 (a – d) shows μEDM waveform with different discharge conditions. It shows that arcing discharge occurs in a continuous set of pulses with a short duration and a smaller current value.

Complete discharge discrimination is difficult by specifying TWR and MRR values for every spark. Bissacco et al. [79] conducted micro-EDM milling experiments while considering electrode wear to address this issue. The smaller quantity of material removed from the electrode compared to the workpiece significantly affected the electrode wear assessment per discharge. This improves the effectiveness of tool wear compensation, which depends on the real-time determination of V_{RT} compared to the electrode. However, an approximation of tool wear error at each discharge will result in an error in the axial depth of the electrode [80]. In addition to counting the complete discharge, the error related to this approximation can be controlled by regularly monitoring the electrode length during machining. During machining, the VRD decreases with increasing depth until it stabilizes at a certain point for a given energy level. Jung et al. [81] presented an indirect real-time μEDM milling TWC technique. Instead of determining electrode wear, the VRD was compensated using an approximation of the work material. The TWC was applied by counting the discharge and compensating according to the VRD of the specimen.

Similarly, Bissaco et al. [82] also implemented compensation for tool wear during micro-EDM milling. VRD presented a reducing path with advancing the machining process and achieving stabilization after a particular depth based on the power range. Jung et al. [83] applied this approach for the first time in μEDM drilling but encountered an error of over 11%. All studies considered pulses to be isoenergetic, and VRD was assumed to remain constant throughout the machining process. However, Bissacco et al. [82] and Nirala et al. [84] had already demonstrated substantial pulse variations during machining with varying depths of micro-EDM, particularly with advanced discharge power. The difference between predicted samples and goal volume compensates the electrode along the Z-axis. However, a steady VRD was used during machining since the pulses were considered isoenergetic. Hoang and Yang [85] replicate a real-time assessment of MRR and sample height. They unveiled that this process elevates the efficiency and productivity of the micro-WEDM (μWEDM) method by augmenting the working capacity of RC circuits. Wang et al. [86] used real-time pulse counting to examine the impact of non-uniform current distributions on EDM material removal and electrode degradation. Their findings revealed that the reverse current could aid in directing debris and shaping the material removal. The number of compensations needed for UWM was determined by Nguyen et al. [40] using real-time monitoring, which provided a more accurate wear assessment than theoretical models.

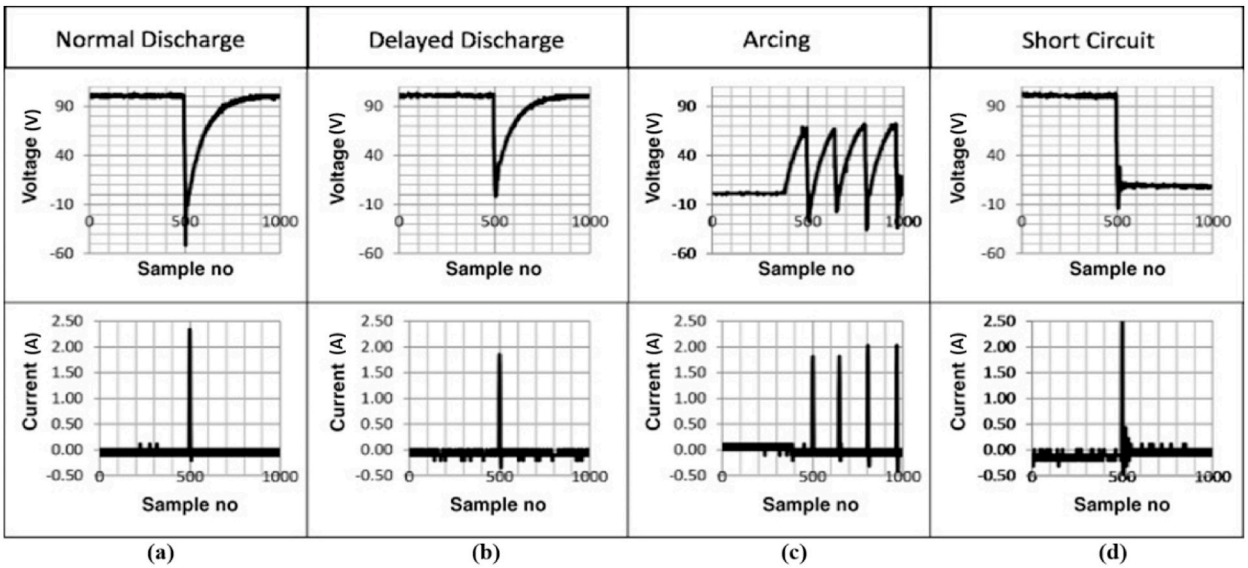

Fig. 22. μEDM waveform with its classification viz., (a) normal discharge, (b) delayed discharge, (c) arcing, and (d) short circuit [23].

4.2. Pulse discrimination-based method

The fraction of normal discharge reduces with increasing machining depth. However, arcing in this situation increases the percentage of delay and short circuits. Eliminating debris from a high aspect ratio hole during machining is a complex task, leading to undesirable debris adhesion to the hole's interior walls. This eventually causes secondary discharge, which prevents the capacitor from fully charging. In this situation, the lower percentage of normal discharge causes a minimum MRR from the workpiece. As previously mentioned, the wear compensation method based on pulse counting did not consider this situation. The drawbacks of the pulse counting method were addressed by introducing a pulse discrimination (PD)-based compensatory system. Many authors have assumed that all μEDM pulses were contributing pulses to remove the material, i.e., isoenergetic. Bissacco et al. [82] found the pulses not to be isoenergetic and claimed that it is crucial to consider non-contributing discharge pulses in the pulse counting method. Nirala et al. [87] and Raza et al. [88] corroborated this claim by conducting a detailed analysis of the discharge pulses, as illustrated in Fig. 23(a–c).

As shown in Fig. 23, it is clear that the nature of discharged and charge pulses varies with the machining depth and hence cannot be considered isoenergetic. This also happens for similar input process parameter settings. Therefore, it is essential to consider the non-contributing character of the pulses when calculating the VRD. To do that, it is crucial to identify various contributing and non-contributing pulse types. This method of determining the pulses tends to develop complete discrimination based on the electrode wear compensation process. To get an accurate V_{RT} in order to fabricate micro rods with the required height, Nirala et al. [89] successfully adapted the real V_{RT} technique to the RμEDM methodology. They employed a similar approach to manufacturing a stainless-steel shadow mask, incorporating batch micro-EDM to produce accurate micro-holes in addition to micro-EDM drilling. They studied various contributing and non-contributing pulses responsible for removing the material. Fig. 24 (a, b) illustrates the voltage discharge pulses recorded throughout the machining operation. In addition, it shows how a threshold value can be used to divide a stream of discharge pulses into a set of contributing and non-contributing pulses. The threshold value used to detect the discharge was 55% of the U_o before it gets discriminated; the rest of the threshold values were decided based on a trial run. Similarly, to discriminate the effective pulses, a limit was fixed at 65%–72%; it was also based on repeated observations that the range delivered adequate energy to remove material. These limitations depend highly on the machining position, making it challenging to be considered normalized.

Nirala and Saha [90] introduced an enhanced VRD method that leverages real-time data to compensate for tool wear. This method approximates V_{RT} from the specimen to conduct TWC instead of directly determining electrode wear. They found that both variants of the necessary depth for microscopic holes were effectively fabricated with errors lower than 4%. Fig. 25 shows the user interface of a pulse discrimination system.

Entire existing approaches were established for a dedicated machine, and using a similar process of pulse discrimination for any other machine needs many changes that made it a difficult task. Nirala et al. [91] proposed a novel pulse-discriminating system that used a simulated signal to demonstrate PD even when the actual machine in operation was inaccessible. Also, they performed pulse discrimination without actual long-running μEDM. As the developer provided one-time simulated or virtual signals similar to the real ones, the problem related to the availability of μEDM to develop the PD system can be solved. Apart from this, PD systems can be more robust because adding variation and noise in simulated signals is relatively easy compared to real ones, which usually depend on machining status. With an improvement in machining, the quick formation of irregular discharges and frequency pulses in the post-machining phase are accepted to give a minimum contribution to removing the material [83,86]. As a result, the various kinds of pulses must be identified before determining VRD. The effectiveness and compensation of the approach built upon active PD have previously been suggested by Liao et al. [76]. They disclosed that the fraction of complex pulses enhances monotonically with drilling depth. Marrocco et al. [92] analyzed μEDM on a composite workpiece with Si3N4–TiN using power spectral density (PSD) analysis. It reveals underlying phenomena governing material removal, surface alterations, and machining efficiency. The unique Si3N4–TiN composition presents challenges, impacting discharge pulse attributes, material removal rates, and surface quality.

Based on pulse counting, Aligiri et al. [23] developed a real-time approach for compensating tool wear during EDM drilling. The specifics of absolute discharge discrimination and material elimination formed the basis of this methodology. Using a thermal model, they computed the volume of debris produced from a single discharge. The author's proposition revolved around quantifying the material removed from the specimen through discharges. Fig. 26 illustrates a diagram of an EDM arrangement that enables real-time monitoring of tool wear compensation.

However, Aligiri et al. [23] also performed electro-thermal modeling for single discharge erosion. For every developed discharge waveform, the pulses on time (T_{on}), regular current during T_{on} and standard voltage during T_{on} were used. To give boundary conditions to the anode, first T_{on} has been utilized to ascertain the radius of the heat source.

The plasma channel's growth has been shown by the heat source's radius and is indicated as a function of T_{on} has been proposed by Patel et al. [93] in 1989, and this is expressed in Eq. (1):

$$R = 0.0633 \times T_{on}^{0.7616} \tag{1}$$

The heat flow radius (R) is shown here in μm, and the T_{on} is shown in nanoseconds. According to Patel et al. [93], the heat flow magnitude (q) is established by Eq. (2) and is supposed to be continuously distributed with time-dependent amplitude:

$$q = \frac{C \times I_a \times V_a}{\pi \times R^2} \tag{2}$$

The dimensionless parameters, such as $= \frac{\alpha \times T_{on}}{R^2}$, $u = \frac{r}{R}$, $w = \frac{z}{R}$, and $\theta(u,w,\tau) = \frac{k_t \times T(r,z,t)}{q \times R}$. According to Carslaw and Jaeger [94], the specimen's material properties are offered to supply a normalized temperature distribution along the vertical axis, and this is expressed

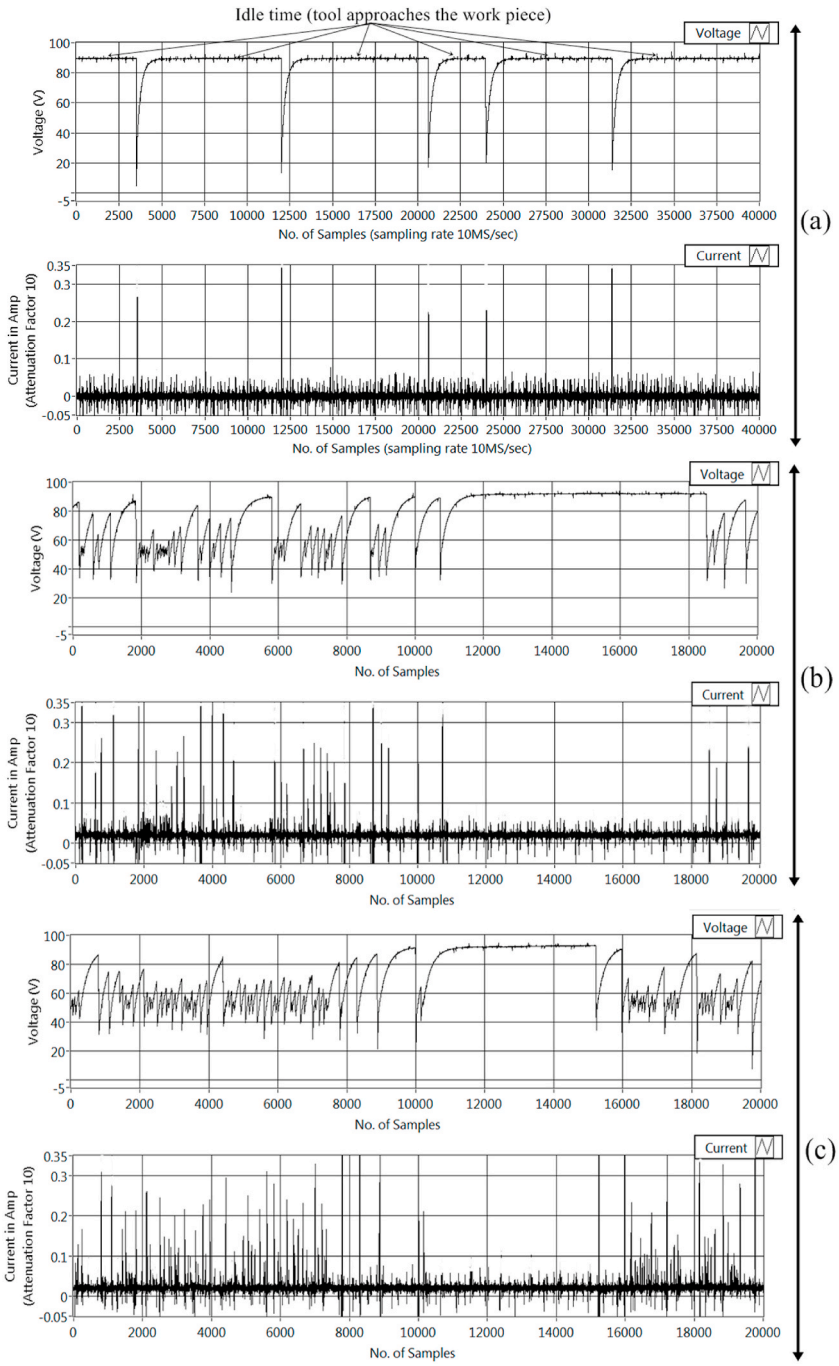

Fig. 23. Pulse events of voltage and current in μEDM drilling at (a) the start, (b) the middle, and (c) the finish [87].

in Eq. 3

$$\theta(0,w,\tau)=\sqrt[2]{\frac{\tau}{\pi}exp\left(-\frac{w^2}{4\tau}\right)}\left[1-\exp\left(-\frac{1}{4\tau}\right)\right]+\sqrt{w^2+1}erfc\left(\frac{\sqrt{w^2+1}}{\sqrt[2]{\tau}}\right)-w\,erfc \tag{3}$$

Yeo et al. [95] provided Eq. (4) to represent the normalized temperature distribution along the horizontal axis:

$$\theta(u,o,\tau)=I_1-I_2 \tag{4}$$

However, Thomas et al. [96] have suggested that the result of the first integral, which they refer to as i.e., I_1 may be stated by Eq.

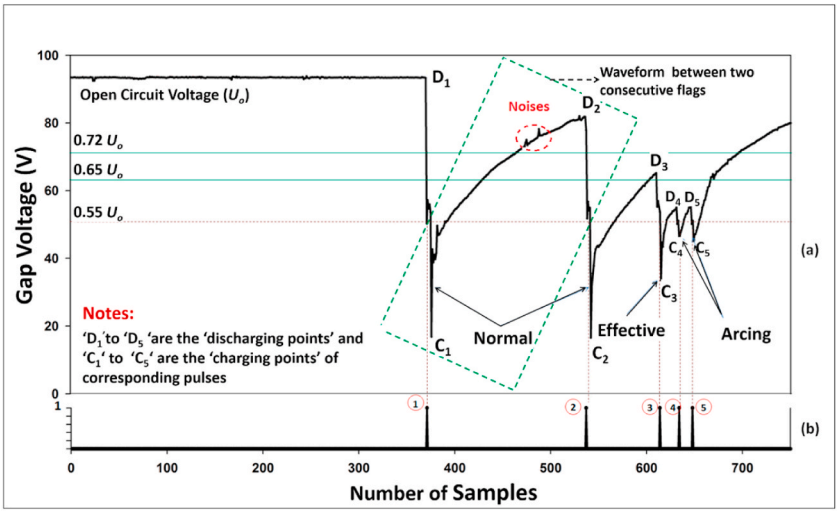

Fig. 24. (a) Typical pulse type in μEDM, (b) Boolean to count pulses [89].

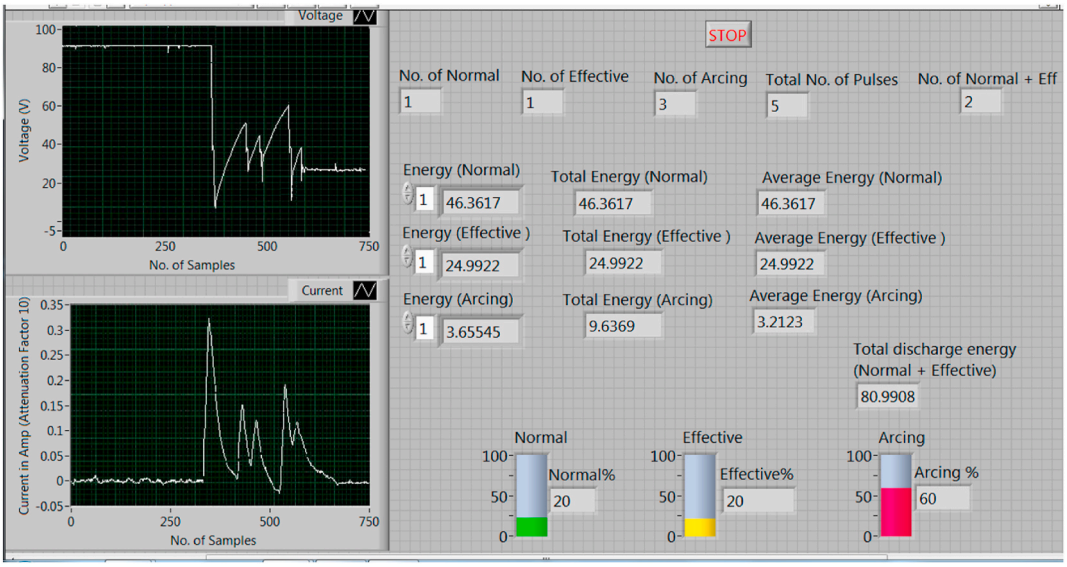

Fig. 25. The front panel of the discriminating pulse system [90].

(5):

$$I_1 = \begin{cases} \dfrac{2}{\pi}E(u), when\ 0 < u < 1 \\ \dfrac{2}{\pi}, when\ u = 1 \\ \dfrac{2u}{\pi}\left[E\left(u^{-1}\right) - \left(1-u^{-2}\right)K\left(u^{-1}\right)\right], when\ u > 1 \end{cases} \tag{5}$$

The elliptical first-type and second-kind integral are denoted in this equation by K and E, respectively. In addition to this, Beck [97] provided a solution to the second kind of integral I_2 and it was written by utilizing Eq. (6):

$$I_2 = \frac{1}{\sqrt[2]{\pi\tau}}\sum_{i=0}^{\infty}\left\{\frac{(-1)^i i!}{(2i+1)(4\tau)^i}\sum_{j=1}^{i+1}(i-j+2)\times\left[\frac{u^{j-1}}{(j-1)!(i-j+2)}\right]^2\right\} \tag{6}$$

Combining the results of Eq. (5) and Eq. (6) in Eq. (4) makes it possible to calculate the dimensionless temperature circulation along the radial axis.

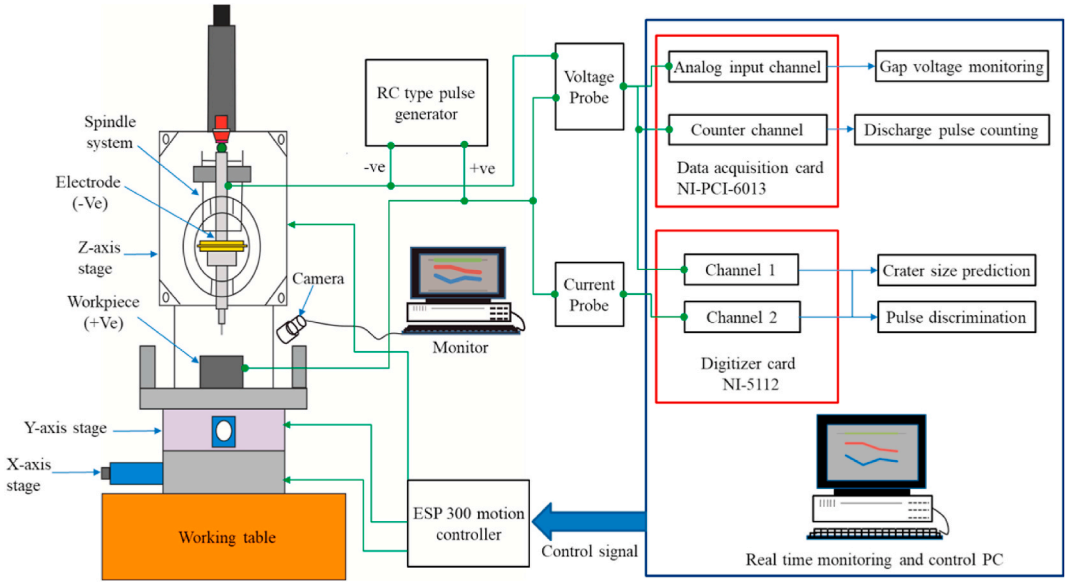

Fig. 26. Schematic of real-time monitoring μEDM system [23].

However, the discharge is not a characteristic of the original method, and the continuous increase in debris needed to be more accurate [82]. A higher accuracy in the electrode wear compensation method was reported by Nirala et al. [98] with the inclusion of regular discharge counts. This PD approach aids in differentiating regular pulses from irregular ones since regular pulses aid in material deterioration. Furthermore, as the μEDM generates non-contributing pulses, the debris volume will provide inaccurately V_{RT}. Related to this, Nadda and Nirala [99] have also concluded that in μEDM, a real-time electrode wear monitoring and compensation approach and a precise thermal model with the least assumptions are necessarily required. μEDM requires a robust pulse discrimination system with some assured potential to discriminate the pulses. The controlled RC-based EDM method was studied by Raza et al. [100–102] for various input variables, including real-time data acquisition, discharge gap, energy per discharge, and MRR. Real-time monitoring and compensating tool wear using a PDS has not been developed for the controlled RC-type power supply, making it a novel and unexplored research area. Developing a controlled RC-type PDS is crucial for comprehending diverse discharge pulses and their influence on MRR while enabling real-time tracking and compensation of electrode wear in EDM. Tee et al. [103] studied PD for the EDM process with a turning tool. They depict a high performance of this process by discriminating the standard pulses from harmful pulses such as short circuits and open circuit pulses based on their determination of delay period. The discharge gap consists of different types of pulses that retain various kinds of information on MRR. Nirala et al. [87] have studied the continuity of processes that depend on evaluating online and offline responses. They revealed that the pulse frequencies in μEDM drilling enhanced from the first to the last part by 125% at smaller alternatives and 133% at more substantial alternatives. While in μEDM dressing, the corresponding values were 55% and 35%, respectively. Fig. 27 depicts the experimental setup's schematic for determining offline and online

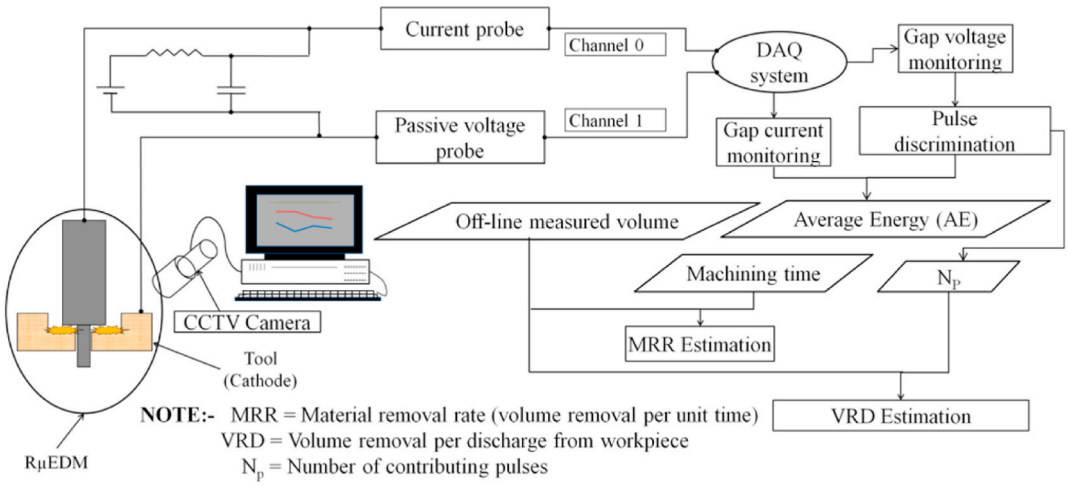

Fig. 27. Schematic and flow chart of innovative setup [87].

outcomes. A comprehensive summary and overview of various tool wear compensation methods proposed by researchers in their investigations and systematic studies in μEDM can be found in Table S1 (supplementary information). A brief summary of online compensation methods in μEDM operations is presented in Table 5.

5. Some other monitoring and compensation methods

The non-linear relationship of the TWR scanning tool is attributed to path overlap, even though the compensation layer is distributed linearly along the tool path in the CLU method. The development of a scanning field method is crucial to effectively address tool wear in specific regions of the tool path. Li et al. [104] introduced a method for compensating tool wear that considers the scanned region on each layer's tool path, enabling continuous compensation of tool wear, as depicted in Fig. 28. The main advantage of this method was the decrease in the occurrence of unusual discharge. The rationale behind incorporating the scanned region along each layer's tool path for continuous tool wear compensation is rooted in achieving a consistent distribution of electrode wear within a single machining layer. The experimental results of the scan field method demonstrated improved MRR and reduced TWR compared to the CLU method.

Lee et al. [105] investigated servo scanning EDM and suggested a 3D machining approach that achieved real-time tool wear compensation through layer-by-layer discharge gap tests. Real-time tool wear correction, CAM system, and inter-servo controls were incorporated into the machining process to attain a consistent depth of cut for each layer. The tool path towards the axial direction was controlled using a servo scanning mechanism, which compares the current and voltage feedback values with discharge condition values to maintain a stable discharge gap [106]. Wang and Dong [107] formulated a model of the micro compressor with a fixed reference compensation method consisting of stator and rotor discs. This involves a simple tool wear compensation method where an electrical connection extracts the coordinate value with a fixed reference point. After machining every layer, the machine coordinate is noted, and the tool's shape is then determined by bringing the tool to a predetermined fixed point. The platinum micro hemisphere was machined to a diameter of 100 μ m by Hang et al. [108]. The longitudinal tool wear compensation coordinates were collected from the dynamic interaction of the electrode with a machined hole and predetermined point source. A compensation method was proposed by Modica et al. [109] to fabricate microchannels with 5–13 mm length and 0.1–0.25 mm depth. The tool's diameter and discharge gap were combined to determine these parameters. Modica et al. [110] used a 400 μm diameter of an electrode with ten control touches to machine a 1 μm thick linear channel. In the primary machining phase, tool wear compensation was not improved due to errors in the work material and alignment. Modica et al. [111] implemented a comparable tool wear compensation method in μEDM milling to fabricate a micro filter mold. By employing this method, the author could fabricate a filter mold comprising 76 pins with a square cross-section of 80 μ m and a height of 0.15 mm. The reference-based compensation method's sole disadvantage is its ability to determine tool wear, and its accuracy is determined by the machine tool's repetition along the z-axis. Moreover, Saraf and Nilara [112] presented a new method for improving Ti6Al4V alloy cutting performance by fabricating unique texture patterns on WC inserts using RμEDM. This technique influences chip formation and reduces tool wear, potentially revolutionizing manufacturing processes. Raza et al. [113] used multiphysics modelling and high-speed imaging validation to study discharge plasma phenomena in μEDM. It uses computational simulations to understand interactions and validate findings with high-speed imaging experiments. This approach improves precision and efficiency in micro-machining applications.

6. Summary and future scopes

This article introduces the intrinsic tool wear those results in dimensional errors in micro-parts produced by EDM and its process variants. Various tool wear, such as longitudinal (axial), circumferential, and corner wear, have been reviewed and identified as invariants of the μEDM process. The review offers a cutting-edge tool wear compensation method to overcome dimensional inaccuracies comprehensively. Real-time tool wear compensation methods employing the PD system as a primary platform are more effective among various approaches for tool wear compensation in μEDM. This is because the real-time strategies consider removing material by each type of discharge pulse with the appropriate fraction obtained by a particular method. Critical to the overall approach, the PD system has been extensively evaluated and deemed suitable for various machining scenarios. The fundamental concerns remain unaddressed, such as the feasibility of implementing the proposed TWC method consistently across a broad range of input process parameters and materials. Recent research indicates that the average percentage error caused by tool wear in the dimensions of the fabricated component could be less than 6% with proper handling. Combining a thermal model-based tool wear compensation method with the current PD system-based approach is recommended as a future direction and has the potential to yield better results. Fig. 29

Table 5
Online compensation methods.

	Methods	Description
Online compensation methods	Pulse counting-based method	This method indirectly counts the number of pulses (without interrupting the machine) while machining. This method compensates for the loss of fluorescence volume from the electrode or workpiece by measuring discharges with a pulse counter.
	Pulse discrimination-based method	This method eliminates the drawbacks of the pulse counting system by introducing a pulse discrimination-based compensatory system. This method avoids the formation of secondary discharge and thus helps the capacitor fully charge.

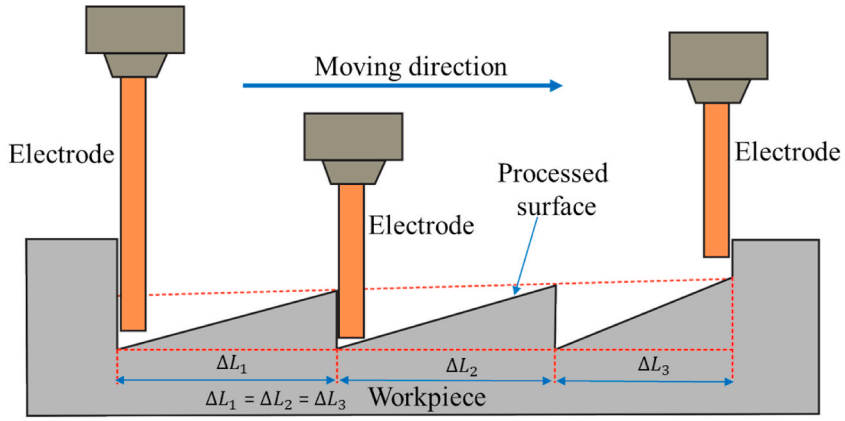

Fig. 28. Schematic of the scanned area tool wear compensation.

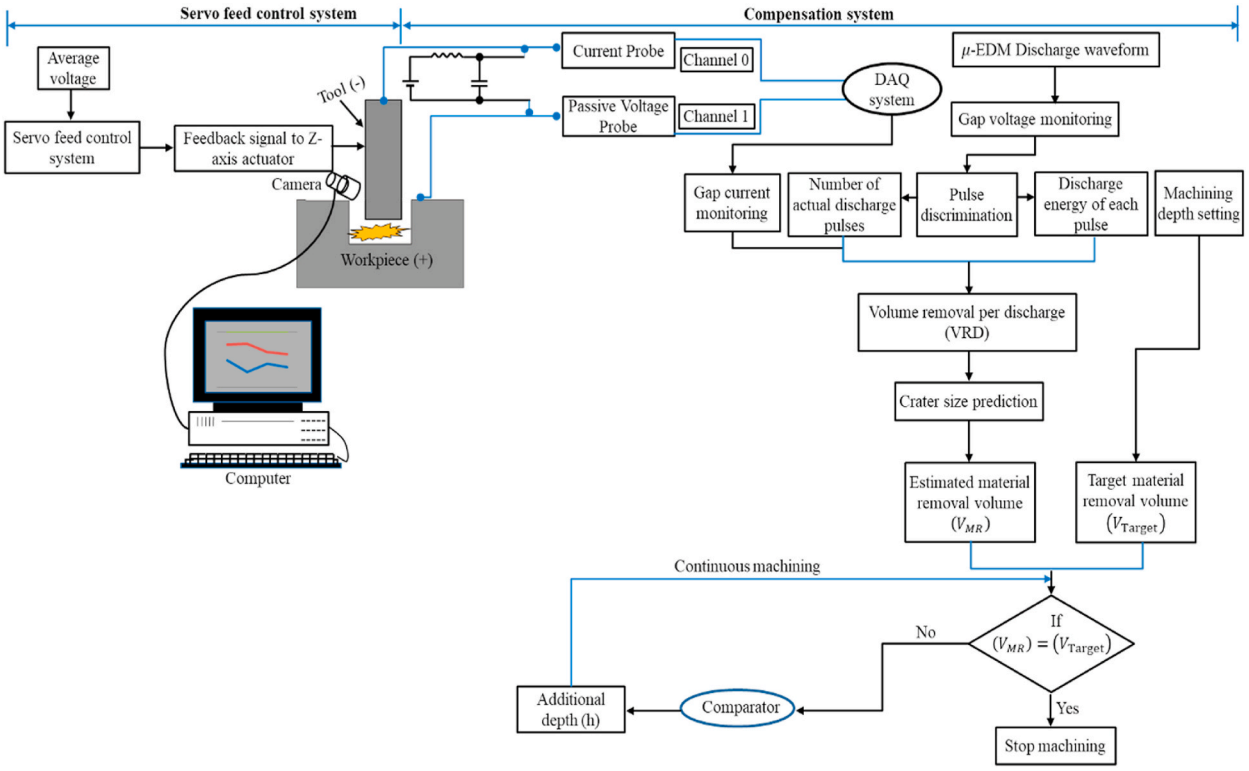

Fig. 29. Proposed schematic for tool wear compensation using a thermal model and PD system-based tool wear compensation approach.

depicts a schematic of the proposed system. This future research direction aims to improve the overall performance and accuracy of μEDM processes while addressing the limitations and challenges of existing tool wear compensation strategies.

Data availability statement

This is a review article; therefore, no data available in the manuscript.

CRediT authorship contribution statement

Rahul Nadda: Conceptualization, Methodology, Data curation, Writing-original draft, Writing-review & editing. **Chandrakant Kumar Nirala:** Conceptualization, Visualization, Writing-review & editing. **Prashant Kumar Singh:** Visualization, Writing-review & editing. **Daeho Lee:** Visualization, Writing-review & editing. **Raj Kumar:** Conceptualization, Visualization, Writing-review & editing.

Tej Singh: Funding acquisition, Data curation, Visualization, Writing-review & editing.

Declaration of competing interest

The authors declare that they have no known competing financial interests or personal relationships that could have appeared to influence the work reported in this paper.

Acknowledgements

The authors gratefully acknowledge the financial support from the Department of Science and Technology (DST) Govt. of India (Grant No. ECR/DST/2017/000918).

Appendix A. Supplementary data

Supplementary data to this article can be found online at https://doi.org/10.1016/j.heliyon.2024.e26784.

References

[1] R. Nadda, C.K. Nirala, Chapter 5 - recent developments in spark erosion–based machining processes: a state of the art in downscaling of spark erosion based machining processes, Editor(s): kapil Gupta, Alokesh Pramanik, in: Handbooks in Advanced Manufacturing, Advanced Machining and Finishing, Elsevier, 2021, pp. 177–215.
[2] R. Nadda, C.K. Nirala, P. Saha, Tool wear compensation in micro-EDM, in: G. Kibria, M. Jahan, B. Bhattacharyya (Eds.), Micro-electrical Discharge Machining Processes. Materials Forming, Machining, and Tribology, Springer, Singapore, 2019, pp. 185–208.
[3] E. Uhlmann, S. Piltz, U. Doll, Machining of micro/miniature dies and molds by electrical discharge machining-Recent development, J. Mater. Process. Technol. 167 (2–3) (2005) 488–499.
[4] B. Bhattacharyya, J. Munda, M. Malapati, Advancement in electrochemical micro-machining, Int. J. Mach. Tool Manufact. 44 (15) (2004) 1577–1589.
[5] J. Mitchell-Smith, I. Bisterov, A. Speidel, I. Ashcroft, A.T. Clare, Direct-writing by active tooling in electrochemical jet processing, Manuf. Lett. 19 (2019) 15–20.
[6] T. Kawanaka, S. Kato, M. Kunieda, J.W. Murray, A.T. Clare, Selective surface texturing using electrolyte jet machining, Procedia CIRP 13 (2014) 345–349.
[7] V.K. Jain, Advanced Machining Processes, Allied Publisher, Delhi, 2002.
[8] J.W. Murray, P.K. Kinnell, A.H. Cannon, B. Bailey, A.T. Clare, Surface finishing of intricate metal mold structures by large-area electron beam irradiation, Precis. Eng. 37 (2) (2013) 443–450.
[9] K. Egashira, T. Masuzawa, Micro ultrasonic machining by the application of workpiece vibrations, CIRP Ann. - Manuf. Technol. 48 (1) (1999) 131–134, https://doi.org/10.1016/S0007-8506(07)63148-5.
[10] F. Boud, J.W. Murray, L.F. Loo, A.T. Clare, P.K. Kinnell, Soluble abrasives for water jet machining, Mater. Manuf. Process. 29 (11–12) (2014) 1346–1352.
[11] J. Mitchell-Smith, A.T. Clare, Electro chemical jet machining of titanium: overcoming passivation layers with ultrasonic assistance, Procedia CIRP 42 (2016) 379–383.
[12] H. Kishore, R. Nadda, C.K. Nirala, A. Agrawal, Modelling and simulation based surface characterization of reverse-μEDM fabricated micro pin-fins, Proc. CIRP. 81 (2019) 1230–1235.
[13] D.K. Chung, H.S. Shin, M.S. Park, C.N. Chu, Machining characteristics of micro EDM in water using high-frequency bipolar pulse, Int. J. Precis. Eng. Manuf. 12 (2011) 195–201.
[14] B.H. Yan, K.L. Wu, F.Y. Huang, C.C. Hsu, A study on the mirror surface machining by using a micro-energy EDM and the electrophoretic deposition polishing, Int. J. Adv. Manuf. Technol. 34 (2007) 96–103.
[15] F. Han, S. Wachi, M. Kunieda, Improvement of machining characteristics of micro-EDM using transistor type impulse generator and servo feed control, Precis. Eng. 28 (4) (2004) 378–385.
[16] K.P. Rjurkar, Z.Y. Yu, 3D micro-EDM using CAD/CAM, Ann CIRP 49 (1) (2000) 127–130.
[17] E.B. Brousseau, S.S. Dimov, D.T. Pham, Some recent advances in multi-material micro and nano-manufacturing, Int. J. Adv. Manuf. Technol. 47 (2010) 161–180.
[18] A.B.M.A. Asad, T. Masaki, M. Rahman, H.S. Lim, Y.S. Wong, Tool-based micro-machining, J. Mater. Process. Technol. 192–193 (2007) 204–211.
[19] R. Nadda, R. Kumar, R. Tej Singh, A. Chauhan, B.G. Patnaik, "Experimental investigation and optimization of cobalt bonded tungsten carbide composite by hybrid AHP-TOPSIS approach, Alex. Eng. J. 57 (4) (2018) 3419–3428.
[20] Z.Y. Yu, K.P. Rajurkar, H. Shen, High aspect ratio and complex shaped blind micro holes by micro EDM, CIRP Ann. - Manuf. Technol. 51 (1) (2002) 359–362.
[21] R. Nadda, C.K. Nirala, Effect of single spark micro-EDM on crater size of different alloys, IOP Conf. Ser. Mater. Sci. Eng. 561 (2019) 012032.
[22] H.L. Yu, J.J. Luan, J.Z. Li, Y.S. Zhang, Z.Y. Yu, D.M. Guo, A new electrode wear compensation method for improving performance in 3D micro EDM milling, J. Micromech. Microeng. 20 (2010) 055011.
[23] E. Aligiri, S.H. Yeo, P.C. Tan, A new tool wear compensation method based on a real-time estimation of material removal volume in micro-EDM, J. Mater. Process. Technol. 210 (15) (2010) 2292–2303.
[24] H. Kurafuji, T. Masuzawa, Micro-EDM of cemented carbide alloys, J. Japan Soc. Electr. Mach. Eng. 2 (3) (1968) 1–16.
[25] Z.Y. Yu, T. Masuzawa, M. Fujino, Micro-EDM for three-dimensional cavities - development of uniform wear method, CIRP Ann 47 (1) (1998) 169–172.
[26] N. Mohri, M. Suzuki, M. Furuya, N. Saito, A. Kobayashi, Electrode wear process in electrical discharge machinings, CIRP Ann. - Manuf. Technol. 44 (1) (1995) 165–168.
[27] Y.H. Jeong, B.K. Min, Geometry prediction of EDM-drilled holes and tool electrode shapes of a micro-EDM process using simulation, Int. J. Mach. Tool Manufact. 47 (12–13) (2007) 1817–1826.
[28] D.T. Pham, A. Ivanov, S. Bigot, K. Popov, S. Dimov, An investigation of tube and rod electrode wear in micro EDM drilling, Int. J. Adv. Manuf. Technol. 33 (2007) 103–109.
[29] W. Kurnia, P.C. Tan, S.H. Yeo, M. Wong, Analytical approximation of the erosion rate and electrode wear in micro-electrical discharge machining, J. Micromech. Microeng. 18 (2008) 085011.
[30] M.P. Jahan, Y.S. Wong, M. Rahman, A study on the quality micro-hole machining of tungsten carbide by a micro-EDM process using a transistor and RC-type pulse generator, J. Mater. Process. Technol. 209 (4) (2009) 1706–1716.
[31] Y. Fu, T. Miyamoto, W. Natsu, W. Zhao, Z. Yu, Study on influence of electrode material on hole drilling in Micro-EDM, Procedia CIRP 42 (2016) 516–520.

[32] M. Hourmand, A.A.D. Sarhan, M.Y. Noordin, Development of new fabrication and measurement techniques of micro-electrodes with high aspect ratio for micro EDM using typical EDM machine, Meas. J Int. Meas. Confed. 97 (2017) 64–78.
[33] R. Kumar, I. Singh, Productivity improvement of micro EDM process by an improvised tool, Precis. Eng. 51 (2018) 529–535.
[34] R. Mehfuz, M.Y. Ali, Investigation of machining parameters for the multiple-response optimization of micro electro discharge milling, Int. J. Adv. Manuf. Technol. 43 (2009) 264–275.
[35] S. Heo, Y.H. Jeong, B.K. Min, S.J. Lee, Virtual EDM simulator: three-dimensional geometric simulation of micro-EDM milling processes, Int. J. Mach. Tool Manufact. 49 (12–13) (2009) 1029–1034.
[36] G. Bissacco, G. Tristo, J. Valentinčič, Assessment of electrode wear measurement in micro EDM milling, in: Proc 7th Int Conf Multi-Material Micro Manuf, 2011, pp. 155–158.
[37] G. Karthikeyan, A.K. Garg, J. Ramkumar, S. Dhamodaran, A microscopic investigation of machining behavior in the μeD-milling process, J. Manuf. Process. 14 (3) (2012) 297–306.
[38] L. Wei, L. Zhang, W. Liu, Z. Jia, A. Li, A new interpolation method of the variable period and step size in micro-EDM milling based on the square constraint, Int. J. Adv. Manuf. Technol. 63 (2012) 621–629.
[39] V.Q. Nguyen, T.H. Duong, H.C. Kim, Precision micro EDM based on real-time monitoring and electrode wear compensation, Int. J. Adv. Manuf. Technol. 79 (2015) 1829–1838.
[40] J. Pei, X. Zhuang, L. Zhang, Y. Zhu, Y. Liu, An improved fix-length compensation method for electrical discharge milling using tubular tools, Int. J. Mach. Tool Manufact. 124 (2018) 22–32.
[41] M. Yamazaki, T. Suzuki, N. Mori, M. Kunieda, EDM of micro-rods by self-drilled holes, J. Mater. Process. Technol. 149 (1–3) (2004) 134–138.
[42] B.H. Kim, B.J. Park, C.N. Chu, Fabrication of multiple electrodes by reverse EDM and their application in micro-ECM, J. Micromech. Microeng. 16 (2006) 843–850.
[43] Y.L. Hwang, C.L. Kuo, S.F. Hwang, Fabrication of a micro-pin array with high density and high hardness by combining mechanical peck-drilling and reverse-EDM, J. Mater. Process. Technol. 210 (9) (2010) 1103–1130.
[44] S.M. Yi, M.S. Park, Y.S. Lee, C.N. Chu, Fabrication of a stainless-steel shadow mask using batch mode micro-EDM, Microsyst. Technol. 14 (2008) 411–417.
[45] W.L. Zeng, Y.P. Gong, Y. Liu, Z.L. Wang, Experimental study of microelectrode array and micro-hole array fabricated by ultrasonic enhanced Micro-EDM, Key Eng. Mater. 364–366 (2008) 482–487.
[46] S. Mastud, R.K. Singh, J. Samuel, S.S. Joshi, Comparative analysis of the process mechanics in micro-electrical discharge machining (EDM) and reverse Micro-EDM, Int. Manuf. Sci. Eng. (2011) 349–358.
[47] S.S. Mujumdar, S.A. Mastud, R.K. Singh, S.S. Joshi, Experimental characterization of the reverse micro-electro discharge machining process for fabrication of high-aspect-ratio micro-rod arrays, Proc. Inst. Mech. Eng. Part B J Eng. Manuf. 224 (2010) 777–794.
[48] S. Mastud, R.K. Singh, S.S. Joshi, Analysis of fabrication of arrayed micro-rods on tungsten carbide using reverse micro-EDM, Int. J. Manuf. Technol. Manag. 26 (2012) 176–195.
[49] M.T. Yan, K.Y. Huang, C.Y. Lo, A study on electrode wear sensing and compensation in Micro-EDM using a machine vision system, Int. J. Adv. Manuf. Technol. 42 (2009) 1065–1073.
[50] T. Kaneko, M. Tsuchiya, Three-dimensional numerically controlled contouring by electric discharge machining with compensation for the deformation of cylindrical tool electrodes, Precis. Eng. 10 (3) (1988) 157–163.
[51] Y. Mizugaki, Contouring electrical discharge machining with on-machine measuring and dressing of a cylindrical graphite electrode, in: Proc. 1996 IEEE IECON 22nd Int Conf Ind Electron Control Instrum, vol. 3, 1996, pp. 4–7.
[52] P. Bleys, J.P. Kruth, Machining complex shapes by numerically controlled EDM, Int. J Electr. Mach. 6 (2001) 61–69.
[53] T. Kaneko, M. Tsuchiya, A. Kazama, Improvement of 3D NC contouring EDM using the cylindrical electrodes-optical measurement of electrode deformation and machining of free-curves, in: Proceedings of the 10th International Symposium for Electro Machining, 1992, pp. 364–367.
[54] J.H. Kim, D.K. Moon, D.W. Lee, J.S. Kim, M.C. Kang, K.H. Kim, Tool wear measuring technique on the machine using CCD and exclusive jig, J. Mater. Process. Technol. 130–131 (2002) 668–674.
[55] R. Guo, W.S. Zhao, L. Li, Z.Y. Li, J.M. Zheng, A micro electrical discharge machining CNC system based on RTAI, Int. Conf. on Integ. Commercialization of Micro and Nanosys. 13 (2009) 1157–1160.
[56] S. Dong, Z. Wang, Y. Wang, J. Zhang, Micro-EDM drilling of high aspect ratio micro-holes and in situ surface improvement in C17200 beryllium copper alloy, J. Alloys Compd. 727 (2017) 1157–1164.
[57] M. Sortino, Application of statistical filtering for optical detection of tool wear, Int. J. Mach. Tool Manufact. 43 (5) (2003) 493–497.
[58] H.S. Lim, Y.S. Wong, M. Rahman, M.K. Edwin Lee, A study on the machining of high-aspect-ratio microstructures using micro-EDM, J. Mater. Process. Technol. 140 (1–3) (2003) 318–325.
[59] J. Jurkovic, M. Korosec, J. Kopac, New approach in tool wear measuring technique using CCD vision system, Int. J. Mach. Tool Manufact. 45 (9) (2005) 1023–1030.
[60] K.Y. Huang, A fast inspection of tool electrode and drilling depth in EDM drilling by detection line algorithm, Sensors 8 (8) (2008) 4866–4877.
[61] M.T. Yan, S.S. Lin, Process planning, and electrode wear compensation for 3D micro-EDM, Int. J. Adv. Manuf. Technol. 53 (2011) 209–219.
[62] T. Yuzawa, T. Magara, Y. Imai, T. Sato, Micro EDM by Thin Rod Electrode, Proceedings of Annual Assembly of Japan Society of Electrical Machining Engineers, 1997, pp. 65–66.
[63] J. Narasimhan, Z. Yu, K.P. Rajurkar, Tool wear compensation and path generation in micro and macro EDM, J. Manuf. Process. 7 (1) (2005) 75–82.
[64] M.S. Puranik, S.S. Joshi, Analysis of the accuracy of high-aspect-ratio holes generated using micro-electric discharge machining drilling, Proc. Inst. Mech. Eng. Part B J Eng. Manuf. 222 (2008) 1453–1464.
[65] J. Wang, J. Qian, E. Ferraris, D. Reynaerts, Precision micro-EDM milling of 3D cavities by incorporating in-situ pulse monitoring, Procedia CIRP 42 (2016) 656–661.
[66] J. Wang, J. Qian, E. Ferraris, D. Reynaerts, In-situ process monitoring and adaptive control for precision micro-EDM cavity milling, Precis. Eng. 47 (2017) 261–275.
[67] K.P. Rajurkar, Z.Y. Yu, Micro EDM can produce micro parts, Manuf. Eng. 125 (5) (2000) 68–75.
[68] J.P. Kruth, P. Bleys, Measuring residual stress caused by wire EDM of tool steel, Int. J Electr. Mach. 5 (2000) 23–28.
[69] J. Pei, Z. Zhou, L. Zhang, X. Zhuang, S. Wu, Y. Zhu, J. Qian, Research on the equivalent plane machining with fix-length compensation method in Micro-EDM, Procedia CIRP 42 (2016) 644–649.
[70] L. Zhang, J. Du, X. Zhuang, Z. Wang, J. Pei, Geometric prediction of a conic tool in micro-EDM milling with fix-length compensation using simulation, Int. J. Mach. Tool Manufact. 89 (2015) 86–94.
[71] L. Zhang, Z. Jia, W. Liu, L. Wei, A study of electrode compensation model improvement in micro-electrical discharge machining milling based on large monolayer thickness, Proc. Inst. Mech. Eng. Part B J Eng. Manuf. 226 (2016) 789–802.
[72] S.M. Wang, H.J. Yu, C.Y. Lee, H.S. Chiu, Study of on-machine error identification and compensation methods for micro machine tools, Meas. Sci. Technol. 27 (8) (2016) 84001.
[73] P. Bleys, J.P. Kruth, B. Lauwers, A. Zryd, R. Delpretti, C. Tricarico, Real-time tool wear compensation in milling EDM, CIRP Ann. - Manuf. Technol. 51 (1) (2002) 157–160.
[74] P. Bleys, J.P. Kruth, B. Lauwers, Sensing and compensation of tool wear in milling EDM, J. Mater. Process. Technol. 149 (1–3) (2004) 139–146.
[75] P. Bhattacharyya, D. Sengupta, S. Mukhopadhyay, A.B. Chattopadhyay, Online tool condition monitoring in face milling using current and power signals, Int. J. Prod. Res. 46 (4) (2008) 1187–1201.
[76] Y.S. Liao, T.Y. Chang, T.J. Chuang, An online monitoring system for a micro-electrical discharge machining (micro-EDM) process, J. Micromech. Microeng. 18 (3) (2008) 35009.

[77] M. Mahardika, G.S. Prihandana, K. Mitsui, Precision machining by discharge pulse counting methods in micro EDM processes, J. Mech. Sci. Technol. 26 (2012) 3597–3603.
[78] S.H. Yeo, E. Aligiri, P.C. Tan, H. Zarepour, A new pulse discriminating system for Micro-EDM, Mater. Manuf. Process. 24 (12) (2009) 1297–1305.
[79] G. Bissacco, H.N. Hansen, G. Tristo, J. Valentincic, Feasibility of wear compensation in micro EDM milling based on discharge counting and discharge population characterization, CIRP Ann. - Manuf. Technol. 60 (1) (2011) 231–234.
[80] G. Puthumana, G. Bissacco, H.N. Hansen, Modelling of the effect of tool wear per discharge estimation error on the depth of machined cavities in micro-EDM milling, Int. J. Adv. Manuf. Technol. 92 (2017) 3253–3264.
[81] J.W. Jung, Y.H. Jeong, B.K. Min, S.J. Lee, Model-based pulse frequency control for Micro-EDM milling using real-time discharge pulse monitoring, J. Manuf. Sci. Eng. 130 (3) (2008) 31106.
[82] G. Bissacco, G. Tristo, H.N. Hansen, J. Valentincic, Reliability of electrode wear compensation based on material removal per discharge in micro EDM milling, CIRP Ann. - Manuf. Technol. 62 (1) (2013) 179–182.
[83] J.W. Jung, S.H. Ko, Y.H. Jeong, B.K. Min, S.J. Lee, Estimation of material removal volume of a micro-EDM drilled hole using discharge pulse monitoring, Int. J. Precis. Eng. Manuf. 8 (4) (2007) 45–49.
[84] C.K. Nirala, P. Saha, Toward the development of a new online tool wear compensation strategy in micro-electro-discharge machining drilling, J Eng. Manuf. 231 (4) (2015) 1–12.
[85] K.T. Hoang, S.H. Yang, A new approach for Micro-WEDM control based on real-time estimation of material removal rate, Int. J. Precis. Eng. Manuf. 16 (2015) 241–246.
[86] J. Wang, F. Yang, J. Qian, D. Reynaerts, Study of alternating current flow in micro-EDM through real-time pulse counting, J. Mater. Process. Technol. 231 (2016) 179–188.
[87] C.K. Nirala, P. Saha, Evaluation of μEDM-drilling and μEDM-dressing performances based on online monitoring of discharge gap conditions, Int. J. Adv. Manuf. Technol. 85 (2015) 1995–2012.
[88] S. Raza, R. Nadda, C.K. Nirala, Discharge pulse analysis based machining responses in vibration assisted μEDM processes, MAPAN 37 (2022) 777–792.
[89] C.K. Nirala, P. Saha, A new approach of tool wear monitoring and compensation in RμEDM process, Mater. Manuf. Process. 31 (4) (2016) 483–494.
[90] C.K. Nirala, P. Saha, Precise μEDM-drilling using real-time indirect tool wear compensation, J. Mater. Process. Technol. 240 (2017) 176–189.
[91] C.K. Nirala, D.R. Unune, H.K. Sankhla, Virtual signal-based pulse discrimination in micro-electro-discharge machining, J. Manuf. Sci. Eng. 139 (9) (2017) 094501.
[92] V. Marrocco, F. Modica, I. Fassi, Analysis of discharge pulses in micro-EDM milling of Si3N4 -TiN composite workpiece by means of power spectral density (PSD), J. Manuf. Process. 43 (2019) 112–118.
[93] M.R. Patel, M.A. Barrufet, P.T. Eubank, D.D. DiBitonto, Theoretical models of the electrical discharge machining process. II. The anode erosion model, J. Appl. Phys. 66 (9) (1989) 4104–4111.
[94] H.S. Carslaw, J.C. Jaeger Conduction of Heat in Solids, second ed., Clarendon, Oxford. .
[95] S.H. Yeo, W. Kurnia, P.C. Tan, Electro-thermal modeling of anode and cathode in micro-EDM, J. Phys. D Appl. Phys. 40 (8) (2007) 2513–2521.
[96] P.H. Thomas, Some conduction problems in the heating of small areas on large solids, Qua. J Mech. and App.Mathem. 10 (4) (1957) 482–493.
[97] J.V. Beck, Large time solutions for temperatures in a semi-infinite body with a disk heat source, Int. J HeatMass Transf. 24 (1) (1981) 155–164.
[98] C.K. Nirala, P. Saha, Towards the development of a new online tool wear compensation strategy in μEDM-drilling, Int. Conf. on Precis.Meso. Micro and Nano Eng. 231 (4) (2017) 588–599.
[99] R. Nadda, C.K. Nirala, Thermal modeling of single discharge in prospect of tool wear compensation in μEDM, Int. J. Adv. Manuf. Technol. 107 (2020) 4573–4595.
[100] S. Raza, R. Nadda, C.K. Nirala, Analysis of Discharge gap using controlled RC based circuit in μEDM process, J Inst Eng India Ser C 103 (2022) 21–27.
[101] S. Raza, R. Nadda, C.K. Nirala, Real-time data acquisition and discharge pulse analysis in controlled RC circuit based Micro-EDM, Microsyst. Technol. (2023) 1–18.
[102] S. Raza, R. Nadda, C.K. Nirala, Sensors-based discharge data acquisition and response measurement in ultrasonic assisted micro-EDM drilling, Meas.: Sens. 29 (2023) 100858.
[103] Ktp Tee, R. Hosseinnezhad, M. Brandt, J. Mo, Pulse discrimination for electrical discharge machining with the rotating electrode, Mach. Sci. Technol. 17 (2) (2013) 292–311, https://doi.org/10.1080/10910344.2013.780559.
[104] J.Z. Li, L. Xiao, H. Wang, H.L. Yu, Z.Y. Yu, Tool wear compensation in 3D micro EDM based on the scanned area, Precis. Eng. 37 (3) (2013) 753–757.
[105] Y. Lee, H. Tong, J. Cui, Y. Wang, Servo scanning EDM for 3D micro structures, in: First International Conference on Integration and Commercialization of Micro and Nanosystems, Parts A and B, ASME, Sanya, Hainan, China, 2007, pp. 1369–1374.
[106] H. Tong, J. Cui, Y. Li, Y. Wang, CAD/CAM integration system of 3D micro EDM. Proceedings of the International Conference on Integration and Commercialization of Micro and Nanosystems, Parts A and B, ASME, Sanya, Hainan, China, MNC2007-21271, pp. 1383-1387. .
[107] Z. Wang, Y. Dong, Micro-EDM milling of micro compressor prototype, in: First International Conference on Integration and Commercialization of Micro and Nanosystems, Parts A and B, ASME, Sanya, Hainan, China, 2007, pp. 1243–1247.
[108] G. Hang, G. Cao, Z. Wang, J. Tang, Z. Wang, W. Zhao, Micro-EDM milling of a micro platinum hemisphere, in: Proc. 1st IEEE Int. Conf. Nano-Micro Eng. Mol. Syst. 1st IEEE-NEMS, 2006, pp. 579–584.
[109] F. Modica, V. Marrocco, P. Moore, I. Fassi, G. Wiens, Al-Mg micro-features using Micro-EDM milling, Aug, in: 6th International Conference on Micro- and Nanosystems; 17th Design for Manufacturing and the Life Cycle Conference vol. 5, ASME, Chicago, Illinois, USA, 2012, pp. 161–167, 12-15.
[110] F. Modica, G. Guadagno, V. Marrocco, I. Fassi, Evaluation of micro-EDM milling performance using pulse discrimination. 19th design for manufacturing and the life cycle 1516 S. KAR AND P. K. PATOWARI conference, in: 8th International Conference on Micro- and Nanosystems, vol. 4, ASME, Buffalo, New York, USA, 2014, pp. 1–8, 17-20.
[111] F. Modica, V. Basile, V. Marrocco, I. Fassi, A new process combining micro-electro-discharge-machining milling and sinking for fast fabrication of micro channels with draft angle, J Micro Nano Manuf 4 (2015) 24501.
[112] G. Saraf, C.K. Nirala, Novel texture pattern on WC inserts fabricated using reverse-μEDM for enhanced cutting of Ti6Al4V, Manuf Lett 36 (2023) 72–75.
[113] S. Raza, H. Kishore, C.K. Nirala, K. Rajurkar, Multiphysics modelling and high-speed imaging-based validation of discharge plasma in micro-EDM, CIRP J. Manuf. Sci. Technol. 43 (2023) 15–29.